STUDIES ON MATHEMATICAL MODELLING OF INFLUENZA IN CANADA

STUDIES ON MATHEMATICAL MODELLING OF INFLUENZA IN CANADA

By

MICHAEL JORDAN DELORME, B.Sc.(H.)

A Thesis

Submitted to the School of Graduate Studies

In Partial Fulfillment of the Requirements

For the Degree

Master of Science

McMaster University

MASTER OF SCIENCE (2010) MCMASTER UNIVERSITY

(BIOLOGY) Hamilton, Ontario

TITLE: Studies on Mathematical Modelling of Influenza in Canada

AUTHOR: Michael Jordan Delorme, B.Sc.(H.) (Queens University)

SUPERVISOR: Dr. Jonathan Dushoff

NUMBER OF PAGES: 71

Abstract

Two studies are presented that involve the mathematical modelling of the 2009/2010 pandemic H1N1 outbreak in Montreal, Quebec, Canada. The first study uses surveillance data and reported vaccination rates to create a model that can recreate the pandemic. The vaccination is then removed from the model and a simulation is run to determine what the pandemic may have looked like without the vaccination campaign. The number of cases, hospitalizations and deaths averted through the vaccination campaign are estimated. The second study recreates both waves of the pH1N1 pandemic by allowing absolute humidity and contacts to change over time. The effect of school re-opening in the fall and the effect of schools not opening in the fall are analyzed. Also, estimates for the reporting efficiency are made for each age group studied. Incorporating absolute humidity changes and the summer school closure allows the model to accurately recreate both incidence waves.

Acknowledgments

Many people have helped me form ideas and complete work throughout my two years at McMaster. I would like to thank the McMaster Biology Graduate Student Society for hosting a research talk where I received some valuable feedback.

To my lab mates; Iilya, Ceda, Audrey, Tallulah, Vik, Xingpeng, Chyun, you have made the long hours in the lab fun and interesting. Thank you for putting up with me and my repetitive requests to play "Guess the Number".

For funding, I would like to thank McMaster, the MITACS Accelerate internship program, the Public Health Agency of Canada, the University of Victoria and the CanPan CIHR Pandemic Influenza Research program.

My experience in Montreal was very valuable to me. I would like to thank the Buckeridge lab and the McGill Clinical and Health Informatics Lab. Also, the Direction de Santé Publique de Montréal provided data, feedback and a great help in shaping the Montreal projects.

This work would not have been possible without the guidance of Drs. Jonathan Dushoff , David Earn and Ben Bolker. They have taught me the importance of being thorough and careful, something that I continue to work on. They have also shared many ideas and experiences with me that I will never forget.

Thank you to my friends and family who have listened to me discuss my research. Thank you to Alison for being supportive of my work and taking care of me.

Table of Contents

List of Figures

Chapter 1

Chapter 2

Figure 11 - Cumulative cases as a proportion of the total population. The solid line is for the model run with school closure for 5-19 year olds. The dashed line is with a Fall semester school closures (children do not return to school for the Fall semester).

Figure 12 - Incident cases as a proportion of the total population: In solid is the model simulation for 5-19 year olds having summer holidays then return to school in the fall. The dashed line is a simulation where children do not return to school after summer vacation.

List of Tables

Chapter 1

Chapter 2

Introduction

Influenza is a virus that causes the deaths and morbidity of thousands of people in Canada every year. Mathematical models of disease allow researchers to explore attributes of different diseases to assess their causes and dynamics. Mathematical models also allow for the prediction and development of possible results of public health interventions.

In this thesis two studies are presented that concern the 2009/2010 pandemic H1N1 outbreak in Montreal, Quebec, Canada. One study uses a mathematical model, surveillance data and vaccination rates to produce an estimate of the impact that the vaccination campaign had. The second study explores the effects of school closure and humidity on the multi-wave structure of the pandemic.

Chapter 1

In this study we use the data collected on laboratory confirmed cases of pH1N1 and the number of vaccines administered to fit parameters to a mathematical model of the disease. The model is then re-run removing all vaccination, as if there were no vaccination campaign at all. The difference between the observed epidemic and the predicted epidemic is used to calculate the numbers of cases, hospitalizations and deaths averted through the vaccination campaign. This method is attractive due to the relatively simple information it requires, such as population size, weekly incidence counts and the level of pre-existing immunity in the population.

We find that the 2009/2010 pH1N1 vaccination campaign in Montreal led to 90 and 436 hospitalizations averted and between 4 and 19 deaths averted. The amount of time between the administration of the vaccine and the onset of protection was found to greatly influence the total reduction in cases. The shorter the time period between when one receives protection following vaccination, the more cases are averted. Compared to instantly receiving protection following vaccination, a delay of 2 weeks prevents 5 times fewer cases. This study can be used to evaluate the effect of the vaccination campaign.

Chapter 2

This study focuses on the causes of the multiple waves of pH1N1 infection that were observed in Montreal. The ending of the first wave and the starting of the second wave appear to be correlated with the timing of the summer school closure and the fall school opening. The timing also seems to correlate with changes in environmental humidity (high humidity, poor influenza virus survival). We combine these factors into a SEIR (Susceptible, Exposed, Infected and Recovered) model to see if they can reproduce the pattern observed through surveillance. The pH1N1 vaccination campaign is also incorporated.

We find that including age structure, changing contact rates and incorporating humidity can allow the mathematical model to produce incidence curves similar to those witnessed in Montreal. The model produces estimates for the level of underreporting of cases for different age groups. The effect of prolonged school closure (continued summer vacation) and prolonged school sessions (no summer vacation) are examined.

Chapter 1

Preface

The following study was completed in collaboration with J. Dushoff and D. Buckeridge. The project was initiated through the CanPan CIHR Pandemic Influenza Research Internship Program and work was conducted at the Clinical and Health Informatics lab at McGill University in Montreal, Quebec. Work was continued at McMaster University.

The Impact of Vaccination During the 2009/2010 pH1N1 Epidemic in Montreal, Quebec, Canada

Delorme, M. J., Dushoff, J. & Buckeridge, D.

Department of Biology, McMaster University, Hamilton Ontario, L8S 4K1

Email: mike.j.delorme@gmail.com

Abstract

The 2009/2010 pandemic of influenza H1N1 is studied using Montreal as the focal population. Data on confirmed cases and weekly vaccination rates are used to construct a mathematical model that can simulate the epidemic in Montreal. The epidemic is then simulated with the effect of the vaccination removed. The estimated number of cases, hospitalizations and deaths averted through the vaccination campaign are found. In total, approximately 921,000 vaccinations are associated with the prevention of between 90 and 436 hospitalizations averted and 4 and 19 deaths averted, depending on the assumed relationship between vaccination and onset of immunity. The results are of interest to public health officials for evaluating the impact of vaccination.

Introduction

In 2009/2010 a new strain of influenza A H1N1 (pH1N1) posed a risk to many people in North America. As with seasonal influenza, vaccination was the main intervention used by public health authorities to control the pH1N1 epidemic. Vaccination benefits individuals both directly, they protect themselves from infection, and indirectly, the spread of the virus is impeded through the effects of herd immunity. The combination of these factors is difficult and expensive to measure using traditional epidemiological

studies where researchers (Nichol *et al.* 1994, Nichol *et al.* 1998, Armstrong *et al.* 2004) evaluate vaccine effectiveness by following cohorts and estimating the extent to which vaccination reduces the risk of infection, hospitalization and death. Our study uses a dynamical disease model and observational data from the population of Montreal to determine the effect of the pH1N1 vaccine.

A unique situation occurred in the fall or "second wave" of the 2009/2010 influenza pandemic when the vaccine was introduced during the course of the epidemic. In North America, seasonal influenza vaccinations are typically administered prior to the start of the flu season in September or October. The pH1N1 vaccine was approved by Health Canada on October 21st 2009 and long manufacturing timelines and post-production testing delayed administration of the vaccine in many North American cities to November 2009. By this point, the initial wave, or "summer wave", of the pH1N1 pandemic had ended in North America and the second wave of infections was occurring in many cities. The effectiveness of a vaccine campaign under different scenarios was prospectively studied (Khazeni *et al.* 2009, Gojovic *et al.* 2009). Khazeni *et al.* (2009) compared possible epidemics and evaluated vaccination campaigns based on differences in R_0, the basic reproductive ratio of the disease. Khazeni's study, along with others (Sander *et al.* 2009) has also prospectively evaluated the economics of different vaccination possibilities.

In this study, we used a dynamical disease model and data on laboratory confirmed cases of pH1N1 to make a direct estimate of the number of infections averted through vaccination. We model the pH1N1 epidemic under different assumptions

regarding the onset of protection following vaccination. The known vaccination rates for Montreal were then incorporated into a mathematical model to generate model parameters. The parameters, fit to the observed epidemic with vaccination, were then used to simulate an epidemic with no vaccination. This method allowed us to estimate the number of infections prevented through vaccination and to calculate the likely number of hospitalizations and deaths prevented.

Methods

Context

We modelled the pH1N1 epidemic in Montreal, Quebec, Canada (assumed constant population size of 1,873,589, Canadian Census 2006) until January 9th 2010. Vaccinations were administered in mass clinics as well as in hospitals and by general practitioners. The first week of vaccination in Montreal was calendar week 42 (the week ending October 24, 2009) although only a few individuals were vaccinated in that week. The mass vaccination campaign ended officially on December 18, 2009 (calendar week 50) and by this point 921,718 vaccinations were administered, over 98% of the eventual total of vaccinations in Montreal. The epidemic was not modeled past the first week of January as the weekly counts of confirmed pH1N1 cases after that date were either 0 or 1. In addition, between January 10, 2010 and May 11, 2010, only an additional 17,550 vaccinations were delivered (Kosal Khun, personal communication).

Data

The data for the number of cases confirmed through surveillance and vaccinations administered from calendar week 36 (the week ending September 12, 2009) to calendar week 1, 2010 (the week ending January 9, 2010) were used to estimate the number of cases averted through the pH1N1 vaccination campaign in Montreal. The data were collected by the Direction de Santé Publique de Montréal (DSP) through their pH1N1 surveillance program. Patients who visited their family physician, flu clinic or hospital were possibly tested for multiple types of influenza infection, including pH1N1. Daily reports were submitted to the DSP. The weekly case counts were found by examining the sampling dates of individuals. After May 15, 2009 in Quebec, testing changed from broad testing to only testing patients with severe sickness (Skowronski *et al.* 2010). This means that there is underreporting in the incidence values for the majority of the epidemic.

The weekly total of lab confirmed cases is an imperfect measure of the true incidence of infection in the population. We used our model to generate an estimate of the case reporting efficiency. For example, a reporting efficiency of 1% means that only 1% of the cases in the population were actually identified and included in weekly surveillance total. This would imply that 1 identified case represents 100 cases in the population. From week 36 (September 12, 2009) to week 1, 2010 (January 9, 2010), there were 2003 lab confirmed cases in Montreal, corresponding under our assumptions to a true incidence of 200,300 cases. We assumed that the reporting efficiency was 1% for the first wave and we fit it as a parameter in our model for the second wave. The estimate of the number of true infections for the first wave was subtracted from the susceptible pool when modelling the second wave.

Model Overview

A modified SIR (Susceptible, Infected and Recovered) model was used to model the disease outbreak (Kermack & McKendrick, 1927). Development of an SIR model requires the initial numbers of infected and recovered people as well as the total population size. A proportion of the population can be presumed immune to pH1N1 at the start of the second wave of and determining the correct size of the susceptible pool is important for the model dynamics (Katriel and Stone, 2009). We adjusted the susceptible pool at the beginning of the second wave to reflect existing immunity in two groups: the elderly with protection from previous influenza exposure and people already infected in the first wave. Cauchemez *et al.* (2009) found that between household contacts, younger people were much more susceptible to infection than older people. The proportion of older people found to be immune to pH1N1 prior to the first wave in the Miller *et al.* (2010) study was approximately 24%. To account for this pre-existing immunity, 24% of the population over 40 was removed prior to the first wave of pH1N1. The sensitivity of our results to this assumption was assessed. We also removed the people who were infected in the first wave (1,278 confirmed cases adjusted for underreporting), since they should have had immunity at the start of the second wave. Therefore, the effective susceptible pool at the start of the second wave was 1,657,757 people. For simplicity, we assume that the vaccine was 100% effective at giving protection. Studies have shown the vaccine to be 70% to 98% effective (Greenberg *et al.* 2009, GlaxoSmithKline Canada 2009, Clark 2009). Lower estimates of vaccine efficacy would lead to the vaccine not preventing as many laboratory confirmed cases, hospitalizations and deaths.

Model Estimation and Validation

The SIR model (Kermack & McKendrick, 1927) was modified and fit to the data on laboratory-confirmed infections reported between calendar week 36 (September 6, 2009) and calendar week 42 (October 24, 2009), the period without vaccination and calendar week 43 (October 31, 2010) to calendar week 1, 2010 (January 9, 2010), the period with the highest vaccination rates. The modification of the SIR model involved removing the Recovered class and adding an equation to track the newly created cases. The parameter values were fit using the mle2 algorithm in R (2.10.0). R_0, the basic reproductive number for the disease, was fit using the susceptible population of Montreal at the start of the second wave. R_0 is the average number of secondary infections caused my one infectious individual in a completely susceptible population. Initial values used for the optimization procedure were R_0=2, δ=2.8 (1/day), I_0=5 (Initial number of infected people in the population) and the case reporting efficiency value was 2%.

$$\frac{dA}{dt} = R_0 \delta \frac{SI}{N}$$

$$\frac{dS}{dt} = -\frac{dA}{dt} - v(t)\frac{S}{N}$$

$$\frac{dI}{dt} = \frac{dA}{dt} - \delta I$$

In the above equations, *v(t)* is the rate at which that vaccinated people leave the susceptible class. The number of incident cases in a week is the difference between *A(t)* and *A(t-1)*. In the above model *N* is the population of Montreal, 1,873,589 (Canadian

Census 2006). We fit R_0, the duration of infectiousness and the initial number of infective people, I_0. The assumed delay from vaccination to full protection was varied so that the model was run with no delay, 1 week delay and 2 week delay scenarios.

Maximum likelihood estimation was done using a Poisson assumption. The optimization method was a broad search over parameter space (method SANN created by Belisle 1992 and coded by Trapletti.) and then a finer search with the parameters returned from the broad search (method Nelder-Mead, Nelder and Mead 1965). The parameter values that were fit were the average duration of infectiousness, R_0, I_0 and the reporting efficiency. This was done for each of the three assumed relationships between vaccination and protection. Standard error values were found using repeated sampling from a multivariate normal distribution after the Nelder-Mead optimization was completed. Overdispersion was evaluated and corrected for by multiplying confidence intervals by the square-root of the overdispersion value. The confidence intervals for the parameters were also corrected. The overdispersion values found for the 0, 7 and 14 delay scenarios were 9.27, 4.22 and 6.20 respectively. We compared the results of these simulations with the surveillance data.

Calculation of Infections Averted

To calculate the possible epidemic without vaccination, the model was first set up to match the observed epidemic and incorporated vaccination. Weekly totals of vaccinations administered were converted to daily vaccination rates. The time from receiving a vaccination to developing protection to pH1N1 was set to 0, 7 and 14 days.

Individuals were removed after vaccination from the susceptible class and parameters were fit to this model. These parameters were then input back into the model and the vaccination rate was set to zero. The resulting epidemics (with and without vaccination) were compared and are plotted in Figures 1, 2 and 3. The 95% confidence intervals for the parameters were found using maximum likelihood analysis with a Poisson assumption and can be found in Table 1. The difference between the two epidemics, the mathematically predicted epidemic without vaccination and the laboratory confirmed curve, is the number of averted cases that can be attributed to the vaccination campaign.

The hospitalization rate for the laboratory confirmed cases as well as the death rate were calculated from records collected by the DSP for the first and second waves of pH1N1 in Montreal. These were used to estimate the number of hospitalizations, cases and deaths averted.

A number of assumptions used in the model were examined including: the value of the reporting ratio for the first wave and the proportion of people immune to pH1N1 prior to the start of the first wave. During the first wave of pH1N1 a higher proportion may have been identified than in the second wave. This difference in identification of cases could be due to changes in testing protocol between the first and second wave, or to changes in patient behaviour in response to the public health messages. This would mean that the reporting efficiency may be lower for the second wave. Assuming lower values for immunity in older people creates a larger susceptible pool at the start of the first and second wave. A larger initial susceptible pool would result in an increase in the predicted number of cases and the estimated number of cases averted would increase.

Results

	R_0	Duration of infectiousness (days)	I_0 – initial number in "Infected" class	Reporting Ratio	Lab confirmed cases averted	Hospitalizations averted	Deaths averted
No delay for protection	1.761 (1.737 to 1.785)	2.528 (2.494 to 2.562)	1.16 (0.49 to 1.83)	32.96 (32.90 to 33.02)	1,553 (1,578 to 1,633)	436 (446 to 459)	19.34 (19.75 to 20.33)
1 week delay	1.753 (1.737 to 1.769)	2.63 (2.507 to 2.753)	2.57 (1.789 to 3.351)	42.83 (42.79 to 42.87)	696 (674 to 718)	195 (189 to 202)	8.66 (8.39 to 8.94)
2 week delay	1.697 (1.677 to 1.717)	2.404 (2.282 to 2.524)	3.372 (2.284 to 4.460)	46.47 (46.42 to 46.52)	320 (300 to 341)	90 (84 to 96)	3.98 (3.74 to 4.25)

Table 1 – Parameter values found through MLE for the three different assumed relationships between vaccination and onset of protection. The range given is the 95% confidence interval for the value.

The results of the model fitting are in Table 1. The data along with the three sets of model output are plotted in Figures 1, 2 and 3. Over the period of the second wave there were 2,003 actual lab confirmed cases. The estimates for the number of cases averted are the differences between the number of cases generated with the model and the estimated true incidence.

The cases averted can also be expressed as a proportion of the population that was susceptible at the start of the second wave. Using the different assumptions between the timing of protection following vaccination, the vaccination campaign in Montreal possibly prevented the infection of up to 2.7% of the total population of Montreal. During this period (Week 42 to week 50) approximately 921,000 vaccinations were administered.

This means that 31 vaccinations were associated with preventing 1 case for the one-week delay scenario.

The hospitalization rate of lab confirmed cases in Montreal for the second wave was approximately 28 hospitalizations per 100 cases. The death rate was approximately 12 deaths per 1000 cases for the same period. Multiplying the estimate of the averted cases by the hospitalization and death rates produces estimates of between 90 and 436 averted hospitalizations and between 4 and 19 averted deaths, respectively. The estimates were calculated by multiplying the hospitalization and death rates by the number of cases averted according to the highest estimate of cases averted for the "no delay" and the lowest estimate from the 14-day delay from vaccination to protection models.

As the assumed delay between vaccination and protection becomes greater, so does the models estimate of the underreporting ratio. The observed pattern is that as the delay from vaccination to protection increases, the R_0 estimate decreases and the case reporting ratio increases.

The assumption that 23% of the population over 40 was not susceptible to pH1N1 infection prior to the first wave was checked. The analysis was repeated with the assumption that 100% of the population over 40 was susceptible prior to the start of the first wave. This was done to test the sensitivity of the pre-existing immunity assumption. This new assumption produced a higher R_0 (3.97 versus 1.73) and a longer duration of infectiousness (4.48 days versus 2.63 days) under the 7 day vaccination to protection delay assumption.

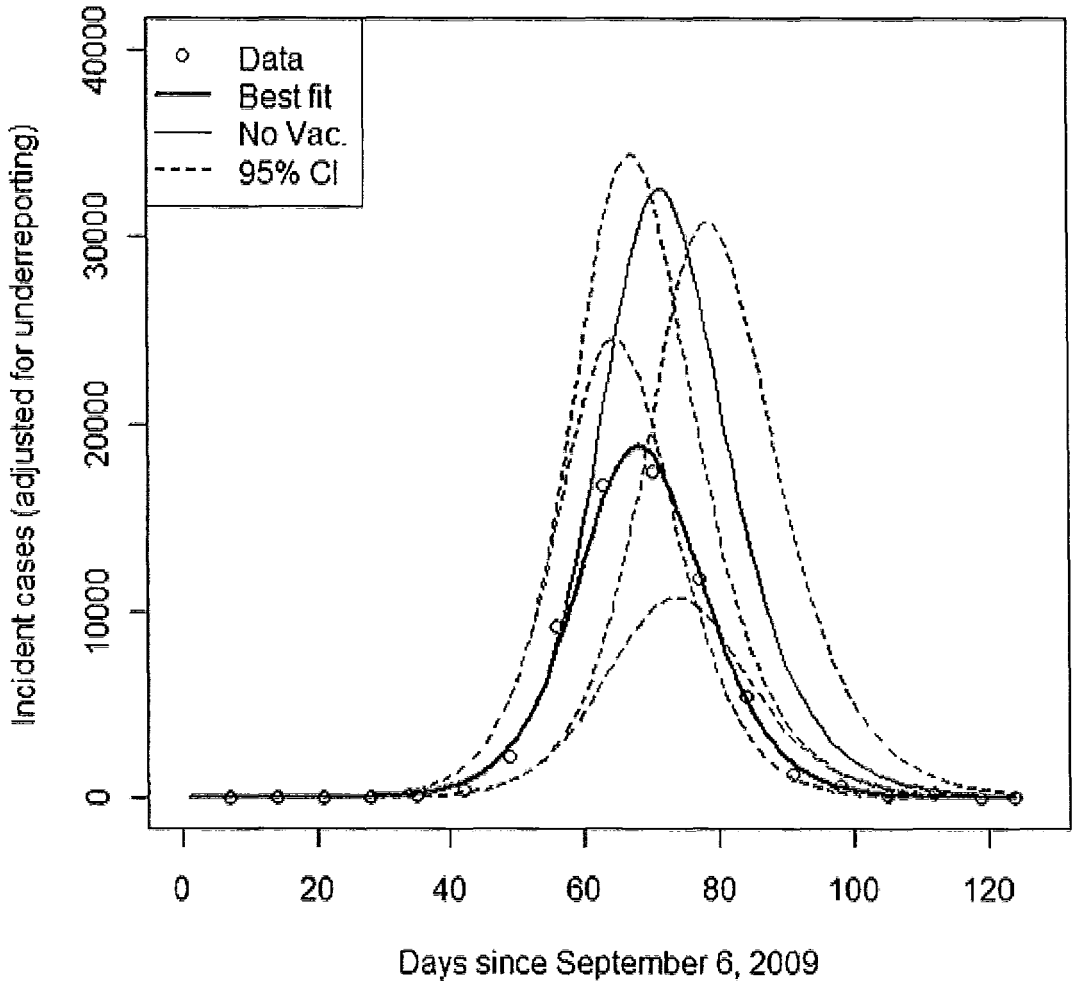

Figure 1 - Simulated epidemic with no delay from vaccination until protection. The open circles are the weekly total of new pH1N1 cases in Montreal, adjusted for underreporting. The thicker solid line is the epidemic simulated using the best fitting parameters. The thinner solid line is the simulated epidemic with no vaccination. The dotted lines are the 95% confidence intervals.

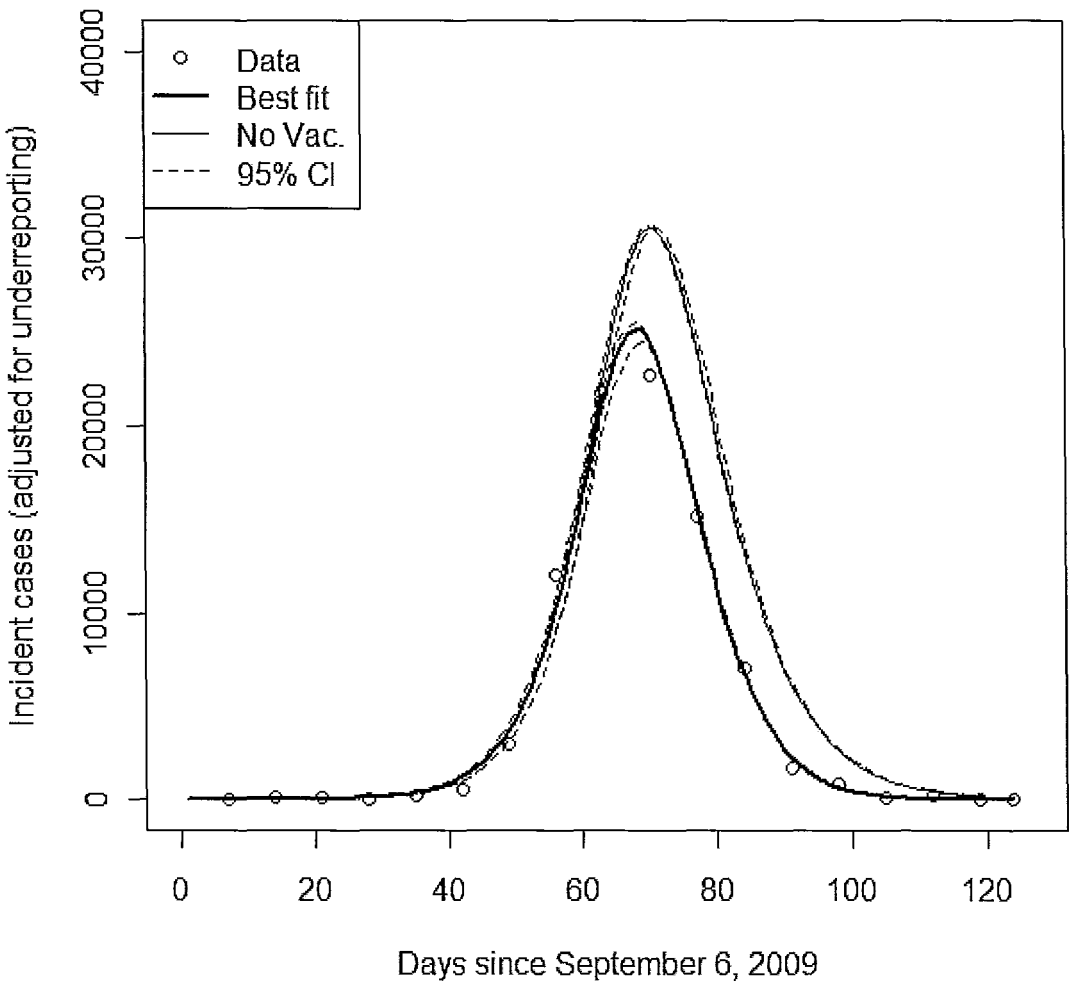

Figure 2 - Simulated epidemic with one week from vaccination until protection. The open circles are the weekly total of new pH1N1 cases in Montreal, adjusted for underreporting. The thicker solid line is the epidemic simulated using the best fitting parameters. The thinner solid line is the simulated epidemic with no vaccination. The dotted lines are the 95% confidence intervals.

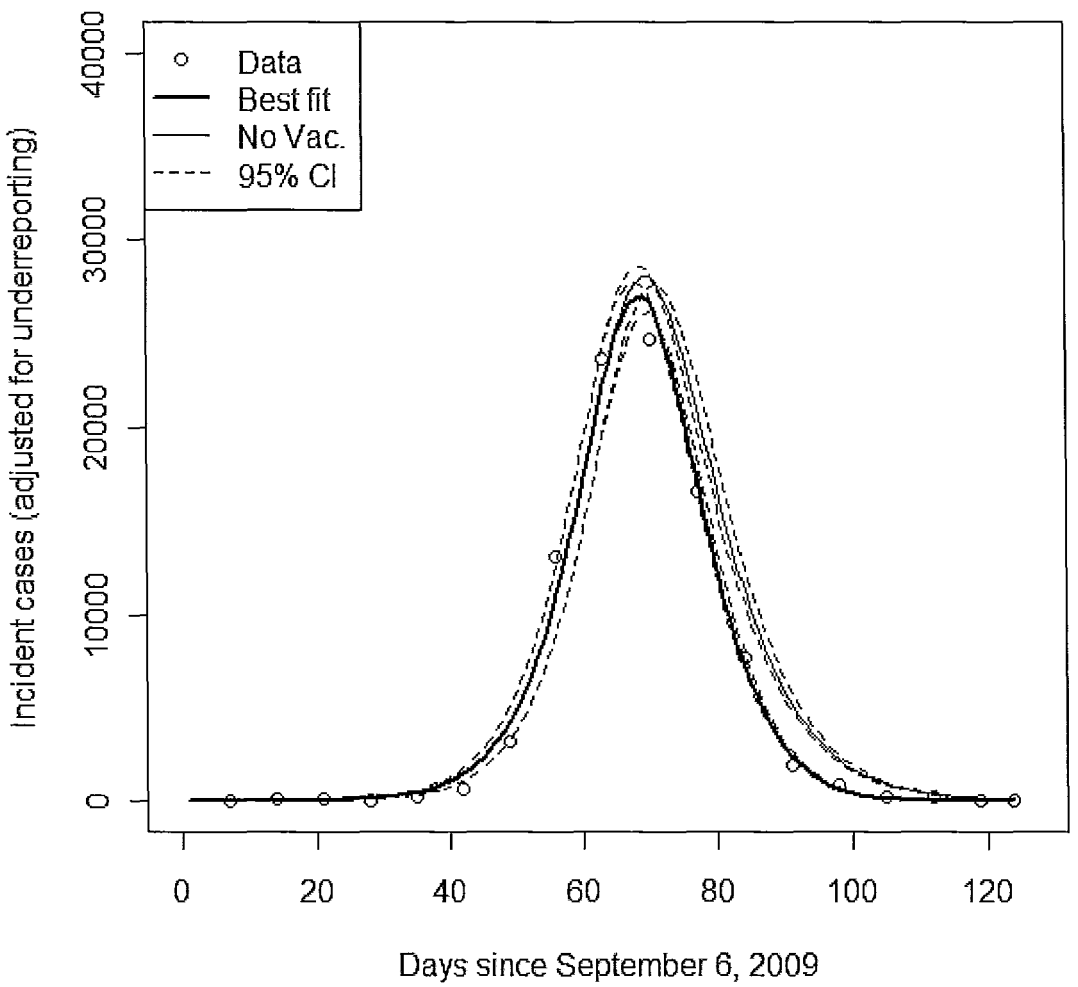

Figure 3 - Simulated epidemic with two weeks from vaccination until protection. The open circles are the weekly total of new pH1N1 cases in Montreal, adjusted for underreporting. The thicker solid line is the epidemic simulated using the best fitting parameters. The thinner solid line is the simulated epidemic with no vaccination. The dotted lines are the 95% confidence intervals.

Discussion

Using a SIR model fit to adjusted incidence and vaccination data we estimated that the approximately 921,000 vaccinations delivered in Montreal were associated with the prevention of up to 1,553 laboratory confirmed cases. Projections from the first wave suggest that these prevented infections would have led up to 436 hospitalizations and 19 deaths. The findings of this study can assist public health policy makers in assessing the benefits of the vaccination program.

The findings also illustrate the importance of the delay between vaccination and effective immunity. It is clear that developing immediate protection following a vaccination would be the best vaccine for stopping new infections. This would immediately remove an individual from the susceptible pool and would lead to the fewer overall cases through reduced transmission caused by population immunity. Assuming a longer delay between vaccination and protection means that individuals remain susceptible for longer, possibly resulting in infection, or infection and transmission of the virus. This study quantifies the difference between a vaccine that delivers immunity quickly and a vaccine that grants immunity one or two weeks after its administration.

It is possible that personal protective measures such as hand washing or antiviral medication may also have contributed to the reduction in cases over the same period that vaccination was occurring. This model does not take into account those factors and assumes that only vaccination was responsible for the overall reduction in cases.

The method used in this study could be applied to a future epidemic where an intervention is available part of the way through an epidemic. A strength of this study is the simplicity of the information used. Population size estimates, weekly case counts and weekly vaccination totals were used to recreate the pH1N1 and account for the benefit gained through vaccination.

Since the timing of the observed cases is consistent between all the simulations, the optimal parameters for the different vaccination scenarios allow for the epidemic to be reproduced with different details. The depletion of susceptible ultimately stops the epidemic in our model. The individuals either move to the recovered class through vaccination or after becoming infected. In the 0 day delay scenario, the parameters that we found show that individuals quickly move from susceptible to recovered through vaccination. In the 14 day delay scenario, individuals quickly move from susceptible to recovered through becoming infected.

The number of cases prevented was found assuming that only vaccination reduces the number of cases. The longer the assumed period from vaccination to onset of immunity, the less benefit is expected for the population (Table 1 and Figure 2). Pourbohloul *et al.* (2009) found R_0 for pH1N1 to be 1.32 (95% CI 1.20 to 1.43) using adjusted data from the initial outbreak in Mexico. A prospective study by Baguelin *et al.* (2010) estimated vaccination rates and vaccine efficacy to find the number of cases, deaths and hospitalizations prevented through vaccination in England. This study found that the number of cases prevented through vaccination corresponds to 4% to 17% of the population of Montreal. Applying the rates found by Khazeni *et al.* (2009), 293 deaths

should be averted in Montreal (we predict 4 to 19 deaths were averted). The difference is likely due to a higher R_0 in the Khazeni *et al.* (2009) study and different assumed vaccination levels. Sander *et al.* (2010) found that the vaccination campaign in Ontario can be associated with preventing 52 pH1N1 deaths, assuming 14 days between vaccination and protection. After adjusting this estimate to Montreal's smaller population size, 7 deaths should be averted in Montreal. This is in line with our corresponding estimate of approximately 4 deaths averted, assuming 14 days between vaccination and protection.

It is possible that factors other than the depletion of susceptible individuals may have caused the number of cases to decrease, but they are not explored here. The largest source of uncertainty is the actual number of cases in the population. The reporting efficiency had to be estimated for this study, but combining multiple data sources may lead to better estimates of the true incidence in the population. Using hospitalization rates instead of (or along with) confirmed pH1N1 cases may lead to reductions in sensitivity caused by the reporting ratio. This approach was not used in this study because of the relatively small number of hospitalizations recorded. The findings of this study can also be used to answer economic questions associated with the vaccination program. The methods used in this study could be applied to other focal cities to assess the impact of regional pH1N1 vaccination campaigns.

Literature Cited

Armstrong, B.G., Mangtani, P., Fletcher, A., Kovats, S., McMichael, A., Pattenden, S. & Wilkinson, P. (2004). Effect of influenza vaccination on excess deaths occurring during periods of high circulation of influenza: cohort study in elderly people. *The British Medical Journal* **329**(7467): 660.

Baguelin, M., Hoek, A. J., Jit. M., White, P. J. & Edmunds, W. J. (2010) Vaccination against pandemic influenza A/H1N1v in England: a real-time economic evaluation. *Vaccine* **28**(12):2370-2384.

Belisle, C.J.P. (1992) Convergence theorems for a class of simulated annealing algorithms on R^d. *Journal of Applied Probability* **29**: 885–895.

Cauchemez, S., Donnelly, C.A., Reed, C., Ghani, A.C., Fraser, C., Kent. C.K., Finelli, L. & Ferguson, N.M. (2009). Household transmission of 2009 pandemic influenza A (H1N1) virus in the United States. *New England Journal of Medicine* **361**(27): 2619-2627.

Clark, T.W., Pareek, M., Hoschler, K., Dillon, H., Nicholson, K.G., Groth, N. & Stephenson , I. (2009) Trial of 2009 influenza A (H1N1) monovalent MF59-adjuvanted vaccine. New England Journal of Medicine **361**(25): 2424-2435.

GlaxoSmithKline Canada. Arepanrix H1N1AS03-Adjuvanted H1N1 pandemic influenza vaccine. Product information leaflet. (2009) Available at: http://www.hc-sc.gc.ca/dhp-mps/prodpharma/legislation/interimorders-arretesurgence/prodinfo-vaccin-eng.php

Gojovic, M.Z., Sander, B., Fisman, D., Krahn , M.D. & Bauch, C.T. (2009). Modelling mitigation strategies for pandemic (H1N1) 2009. *Canadian Medical Association Journal* **181**(10): 673-80.

Greenberg, M. E., Lai, M. H., Hartel, G. F., Wichems, C.H., Gittleson, C., Bennet, J., Dawson, G., Hu, W., Leggio, C., Washington, D.& Basser, R.L. (2009) Response to a Monovalent 2009 Influenza A (H1N1) Vaccine. *New England Journal of Medicine* **361**:2405-2413.

Institut de la statistique Quebec. Population by age group, Montreal and Laval administrative regions, 2006 Statistics Canada, 2006 Census of Canada. Accessed March 3, 2009.

Katriel, G. & Stone, L. (2009). Pandemic dynamics and the breakdown of herd immunity. *PLoS Currents Influenza* RRN1046.

Kermack, W. O. & McKendrick, A. G. (1927) A contribution to the mathematical theory of epidemics. Proceedings of the Royal Society of London, Series A, **115**:700–721.

Khazeni, N., Hutton, D. W., Garber, A. M., Hupert, N. & Douglas K. O. (2009) Effectiveness and Cost-Effectiveness of Vaccination Against Pandemic Influenza (H1N1) 2009. Annals of Internal Medicine **151**: 829-839.

Miller, E., Hoschler, K., Hardelid, P., Stanford, E., Andrews, N. & Zambon, M. (2010) Incidence of 2009 pandemic influenza A H1N1 infection in England: a cross-sectional serological study. *Lancet* **375**(9720):1100-1108.

Nelder, J. A., and Mead, R. (1965) A simplex algorithm for function minimization. *Computer Journal* **7**: 308–313.

Nichol, K. L., Margolis, K. L., Wuorenma, J. & Von Sternberg, T. (1994) The efficacy and cost effectiveness of vaccination against influenza among elderly persons living in the community. New England Journal of Medicine **331**(12): 778-784.

Nichol, K. L., Wuorenma, J. & von Sternberg, T. (1998) Benefits of influenza vaccination for low-, intermediate-, and high-risk senior citizens. *Archives of Internal Medicine* **158**(16):1769-1776.

Pourbohloul, B., Ahued, A., Davoudi, B., Meza, R., Meyers, L. A., Skowronski, D. M., Villaseñor, I., Galván, F., Cravioto, P., Earn, D. J., Dushoff, J., Fisman, D., Edmunds, W. J., Hupert, N., Scarpino, S. V., Trujillo, J., Lutzow, M., Morales, J., Contreras, A., Chávez, C., Patrick, D. M. & Brunham, R. C. (2009) Initial human transmission dynamics of the pandemic (H1N1) 2009 virus in North America. *Influenza and Other Respiratory Viruses* **3**(5):215-222.

Reed, C., Angulo, F. J., Swerdlow, D. L., Lipsitch, M., Meltzer, M. I., Jernigan, D. & Finelli, L. (2009) Estimates of the prevalence of pandemic (H1N1) 2009, United States, April-July 2009. *Emerging Infectious Diseases* **15**(12):2004-7.

Sander, B., Bauch, C., Fisman, D. N., Fowler, R., Kwong, J. C., McGeer, A., Zivkovic, G. M. & Krahn, M. (2009) Is a Mass Immunization Program for Pandemic (H1N1) 2009 Good Value for Money? Early Evidence from the Canadian Experience. *PLoS Currents Influenza* RRN1137.

Skwronski, D.M., De Serres, G., Crowcroft, N.S., Janjua, N.Z., Boulianne N., Hottes, T.S., Rosella, L.C., Dickinson, J.A., Rodica, G., Sethi, P., Ouhoummane, N., Willison, D.J., Rouleau, I., Petric, M., Fonseca, K., Drews, S.J., Rebbapragada, A., Charest, H., Hamelin, M., Boivin, G., Gardy, J.L., Li, Y., Kwindt, T.L., Patrick, D.M., Brunham R.C. and for the Canadian SAVOIR Team. (2010)

Association between the 2008–09 Seasonal Influenza Vaccine and Pandemic H1N1 Illness during Spring– Summer 2009: Four Observational Studies from Canada. *Public Library of Science Medicine* 7(4): e1000258. doi:10.1371/journal.pmed.1000258.

Tuite, A. R., Greer, A. L., Whelan, M., Winter, A. L., Lee, B., Yan, P., Wu, J., Moghadas, S.,Buckeridge, D., Pourbohloul, B. & Fisman, D. F. (2010) Estimated epidemiologic parameters and morbidity associated with pandemic H1N1 influenza. *Canadian Medical Association Journal* **182**(2):131-6.

Chapter 2

Preface

The following study was completed in collaboration with C. Rozins, J. Dushoff and D. Buckeridge. The project was initiated through the CanPan CIHR Pandemic Influenza Research Internship Program and work was conducted at the Clinical and Health Informatics lab at McGill University in Montreal, Quebec. C. Rozins was involved in the study concept and design, the coding of the model and drafted the manuscript. Michael Delorme was involved in the study concept and design, gathered and formatted the surveillance data, interpreted the results and drafted the manuscript.

Examining Possible Determinants of the Multiple Wave Structure of Pandemic Influenza

Rozins, C., Delorme, M. J., Dushoff, J. & Buckeridge, D.
Department of Biology, McMaster University, Hamilton Ontario, L8S 4K1

Email: mike.j.delorme@gmail.com

Abstract

In 2009/2010 pandemic influenza emerged in numerous countries around the world. Similarly to pandemics in the past, the most recent outbreak appeared in multiple waves. Increasing our understanding of the possible determinants of the multiple wave structure is beneficial to public health. We model both waves of the 2009/2010 outbreak with a single age structured compartmental model. We incorporate environmental humidity and the school calendar into our model. Using confirmed cases and vaccination figures provided by the Direction de Santé Publique de Montreal, we are able to estimate unknown parameter values. We show that with the addition of two simple features to the basic SEIR model we can produce multiple waves that match the recent outbreak well. With our multi-wave model we then go on to simulate different school closure scenarios and show that summer holidays decrease the total epidemic size and delaying the return of children back to school will substantially decrease the epidemic size.

Introduction

Influenza pandemics are typically caused when an antigenically different strain of influenza emerges and spreads globally due to the high level of susceptibility in the population. This study examines the 2009/2010 pandemic H1N1 influenza (pH1N1) in

Montreal. One key characteristic observed in pandemic influenza is the tendency for incidence in the population to cycle (Miller *et al.* 2009). Theory indicates that the initial spread is due to the susceptibility of the host population but the causes of subsequent waves are not well understood. There were multiple waves of incidence in the 1918 flu pandemic, 1957 pandemic and the 1968 pandemic (Miller *et al.* 2009). Some theories suggest that genetic drift in the influenza virus can cause individuals to become susceptible; others a link between vitamin D deficiency and innate immunity while others argue the waves are triggered by environmental factors (Reid *et al.* 2001, Cannell *et al.* 2008, Shaman & Kohn 2009, Lowen *et al.* 2007). Few studies have looked at combining these factors and using them in a model. Understanding the dynamics of the epidemic leads to better strategies for influenza control. Dynamical models can lead to better case forecasting programs and ultimately better intervention policies.

Recently, a number of papers investigating factors such as temperature, relative humidity and absolute humidity (AH) and their roles in influenza virus survival and transmission have emerged (Shaman & Kohn 2009, Lowen *et al.* 2007). Shaman and Kohn (2009) found that in temperate regions influenza virus transmission and survival are more tightly constrained by absolute humidity than by relative humidity or temperature. It is unknown however, if the multiple waves of incidence during an influenza pandemic can be completely explained by environmental factors. In this paper we do not address other hypotheses for the cause of pandemic waves such as viral mutation or the loss of susceptibility by individuals (Lipsitch & Viboud 2009). We also do not specifically attribute seasonality to vitamin D production or spending more time indoors in the winter

in our model. Increased vitamin D production may lead to improved immune system functioning and fewer new infections, but this can be encapsulated in the changes of the transmission of the virus. Spending more time indoors may be coupled with increased contact rates and more opportunities for infection to occur. The only contact rate that we change in our study is the rate of children interacting with children.

It has been well documented that school-aged children contribute substantially to the initial spread of an epidemic (Wallinga *et al.* 2006, Mossong *et al.* 2008, Longini *et al.* 1982). Contacts between school-age children with individuals of the same age group are more frequent than in any other age group. Vaccination of school-aged children and young adults should be a priority if a vaccine is available before the main outbreak (Medlock & Galvani 2009, Ferguson *et al.* 2006). The type of physical contact between school-aged children also facilitates increased viral spread (Mossong *et al.* 2008).

From a biological point of view, there are a number of factors that could contribute to the multiple waves of incidence in a pandemic. We focus our attention on the factors which we believed would have the greatest effects. Not only did incidence in the population decrease dramatically in the late spring of 2009, but incidence remained extremely low until the fall of 2009. Mathematically, if there is a drastic change in the probability of infection (given a contact), or a drastic change in the average number of contacts between individuals, the spread of infection in the population could decrease or even cease completely, leaving a large susceptible pool untouched by the infection.

The simplest epidemic models are only capable of modeling a single incidence wave at a time and do not include multiple age groups. The simple models place individuals into categories based on the disease state of the individual. Also, static transmission rates produce single waves of disease that end once the susceptible population has been depleted. We derive a model that is capable of producing multiple waves of incidence and allows multiple factors to contribute to the growth and decline of incidence values. According to the weekly incidence values reported and the relative size of the population of Montreal, at the end of the first wave a large proportion of the population was still susceptible. This indicates that depletion of susceptible individuals is likely not what caused the disease to taper off. By including environmental factors and school calendar induced contact changes in a simple SEIR model (Susceptible, Exposed, Infectious and Recovered), we obtain a model that is capable of producing multiple waves of incidence without depleting the majority of the susceptible individuals in the population until the end of the pandemic. We examine two potential causes of the multiple wave structure because we are attempting to get a more complete assessment of the roles that each has. Also, we are able to examine strategies that we have control over (school closure timing) and its interaction with a factor that we do not generally have control over (absolute humidity).

We included age structure in our model. Not only because it helps alleviate the bias associated with oversimplifying human interactions for the sake of modeling but also because each age group has unique characteristics that play an important part in the course of the pandemic. We used the age groups 0-4 years, 5-19 years, 20-39 years and

40+ years. It has been well documented that the actions of school-aged children are strong factors which drive the initial stages of a pandemic (Mossong *et al.* 2008, Wallinga *et al.* 2006). Surveillance indicates that younger individuals were infected at higher rates than what are typically observed with seasonal influenza. During a disease outbreak one of the immediate goals that public health officials have is to identify what groups are being affected the most. We should examine multiple age groups because the public health response should depend on who is getting sick. The vaccination program in Montreal was structured on the assumption that targeting different age groups would be the best approach to decrease the burden of the disease. Medlock *et al.* (2010) explored the effects of vaccinating different age groups with a vaccine that becomes available mid-pandemic. They found that vaccinating high risk people and school-aged children should be the first priority to reduce pH1N1 deaths (Medlock *et al.* 2010) We also know that some proportion of the "older" population has some resistance to infection hypothesized to be due to previous exposure to similar influenza viruses during their lifetime (Hancock *et al.* 2009, Fisman *et al.* 2009). The last influenza pandemic struck in 1968 and 1969, approximately 40 years ago. It was important for us to separate this group of individuals from the rest of the population since they have some resistance to the new pH1N1 virus in circulation. We removed 23% of the 40+ age group to reflect the level of pre-existing immunity to pH1N1 prior to the start of the first wave (Miller *et al.* 2010).

Clinical Reporting

All data on weekly case counts was gathered by the Direction de Santé Publique de Montreal (DSP). We sort the weekly laboratory confirmed cases into the respective

age group to get weekly incidence. We assume that the day the sample was collected from the patient is the day that the individual became infectious. It is very likely that the number of confirmed pH1N1 cases is a substantial underestimate of the total number of illnesses that actually occurred in the population (Reed *et al.* 2009). The reporting efficiency may be low for a number of reasons (Reed *et al.* 2009). Not all ill people seek medical care and have a specimen collected. Not all specimens collected get sent to the public health laboratories and not all specimens from infected people will give a positive test result possibly because of the timing of the collection or the quality of the specimen (Reed *et al.* 2009). After May 15 in Quebec, testing was restricted from sentinel physicians to patients with severe illness (Skowronski *et al.* 2010). This means that after 3 weeks of the identification of the initial cases in Montreal the level of influenza subtype testing decreased. This causes there to be underreporting in the incidence values for the majority of the epidemic. Multiplying the number of officially recorded cases to estimate the true incidence of disease in the population is not a novel method. Low reporting efficacy values mean that one emergency room visit or one lab confirmed specimen represents many infections in the population. A New York based study estimated the number of cases in the population represented by one emergency room visit. It was found that one visit by an adult aged 18-64 represented 76.5 cases in the population and one visit by an adult over 65 represented 11.1 cases in the population (Metzger *et al.* 2004). It has been estimated that one lab confirmed case of pH1N1 infection could represent as many as 140 infected people in the population (Reed *et al.* 2009).

Methods

We modeled the 2009/2010 influenza pandemic in Montreal with an age-structured SEIR model modified to include absolute humidity. We incorporated seasonality in transmission and changes in school-aged contacts during the summer holidays into the model. With these few changes and initial conditions, vaccination data and weather data specific to Montreal, Canada, we derived a model capable of simulating both waves of the pandemic. Montreal, Canada is a densely populated city in Eastern Canada with a total population, according to the 2006 census, of approximately 1.85 million people (Institut de la statistique Quebec 2006).

The Model Overview

Our model treats the population as if it were divided up into compartments. At all times, for each age group α there are compartments for susceptible individuals (S_α), exposed individuals (E_α), infectious individuals (I_α) and removed/recovered individuals (R_α). Susceptible individuals become infected when they come in contact with an infected individual, governed by a transmission rate. Once an individual becomes infected, there is a latent period in which they are unable to spread the infection to others and do not show any symptoms. This period of time is referred to as the "exposed period". After a sufficient amount of time in the exposed period, the individual leaves the class and becomes infectious. From the infectious class, the individual eventually recovers and moves onto the removed class, where they are no longer infectious and are immune to infection. Because we are investigating a single pandemic which took place over a period

of less than a year, we chose not to include natural deaths, births or loss of immunity in our model. We do not include disease deaths in our model since the total number of confirmed pH1N1 deaths was low relative to the population size. The complete age structured model has four compartments for disease state of the individual with four distinct age groups within each disease state, giving us a total of 16 equations. Since each population size is fixed, the 16 equations can be reduced to 12 independent equations.

Transmission Rate

In our model we have allowed transmission to vary over the course of the epidemic by incorporating age-based contact rate changes and the effect of environmental humidity on influenza virus transmission. A successful transmission of the virus from one individual to another is dependent upon two factors, weekly effective social contacts C_{ij} and the vapour pressure coefficient β_t. As the absolute humidity increases, the transmission rates decrease. We used the daily average relative humidity (RH) and temperature to calculate the daily average vapour pressure using the Clausius-Clapeyron relation (Equation 1). We use vapour pressure as a measure of the absolute humidity in Montreal (Shaman & Kohn 2009). We calculate the saturation vapour pressure $\rho_{s(t)}$ at temperature T. $\rho_{s(T0)}$ is the saturation vapour pressure at a reference temperate T_0, L is the latent heat of evaporation for water and R_v is the gas constant for water vapour (Shaman & Kohn 2009). The vapour pressure, ρ, is then calculated using the saturation vapour pressure and RH (Shaman & Kohn 2009).

$$\rho_s(T) = \rho_s(T_0) \times \exp\left(\frac{L}{R_v}\left(\frac{1}{T_0} - \frac{1}{T}\right)\right)$$
$$\rho = \rho_s(T) \times \frac{RH}{100} \quad (1)$$

We then scaled ρ_t to be between zero and one and set $\beta_t=exp(-y\rho_t)$, where y is an estimated parameter that converts reduced vapour pressure to increased transmission of the virus. Below we show the incidence rate, Λ, for a specific age group α. The contact rate is assumed to be proportional to the product of the sizes of the susceptible and the infectious groups S_α and I_α respectively.

$$\Lambda_\alpha = \beta_t S_\alpha \sum_{\alpha'} C_{\alpha,\alpha'} I_{\alpha'} \quad (2)$$

Contact Matrix

The C_{ij} in the incidence rate equation is a matrix containing contact parameters for each age group representing the effective contact rate. The rows of the contact matrix represent susceptible individuals and the columns represent infectious individuals. An individual entry c_{ij} represents the average number of weekly contacts between a susceptible *i* individual with infected individuals of age group *j*. The parameter *k* (below) corresponds to the time period of the pandemic.

$$C_{ij} = \begin{vmatrix} a & b & b & b \\ b & c_k & b & b \\ b & b & a & b \\ b & b & b & a \end{vmatrix}, \quad k = 1, 2, 3$$

For simplicity we assumed that individuals of different age groups mix at a constant rate, *b* and individuals in the same age group mix at a constant rate *a*. It is known that people are most likely to interact with individuals who are close in age (Wallinga *et al.*2006). Using a previous study, we were able to scale the values in our contact matrix, C_{ij}. The social contact data in Wallinga *et al.* (2006) was obtained from a survey in the town of Utrecht in the Netherlands (Wallinga *et al.* 2006). We took their normalized contact matrix and scaled it down to 4 age groups, closely resembling our age group sizes. Then we averaged over the two types of interactions described earlier: 1) contacts with individuals in your own age group *a* and 2) contacts with individuals in other age groups *b*. When calculating the average within group contact rate, *a*, we excluded the school-aged children. Now we have reduced the matrix down to three values, *a*, *b* and *c*, but we can express *b* and *c* as multiples of *a*. Instead of having 16 unique entries in the 4X4 contact matrix, all of the values are scaling of *a*. This leaves one contact parameter, *a,* to be fit to the data.

In our model school-aged children, age 5-19, do not mix at rate *a*, but mix at a rate c_k. It has been well documented that school-aged children come in contact with individuals of their own age group more than any other age group mixes with itself or with other age groups (Wallinga *et al.* 2006, Mossong *et al.* 2008). Because of the

increased contacts, school-aged children are typically strong drivers of pandemics (Mossong *et al.* 2008). We assume that school-age children come in contact with individuals of their own age group more often during the school year when they are more aggregated in schools (Bjørnstad *et al.* 2002). To implement this assumption we change the contact rates of school-aged children during the summer holidays and when they return to school, thus the requirement for three contact parameters, c_1, c_2 and c_3. We have made the assumption that

$$c_1 = c_3 > c_2 = a > b$$

where c_1 is the contact rate between school-aged children during the spring 2009 semester, c_2 is the contact rate between school-aged children during the summer holidays and c_3 is the contact rate between school-aged children during the fall 2009 semester. The makeup and changes in the contact matrix are difficult to know accurately. We feel that our simplified contact matrix is a fair substitute for having reliable contact data and incorporates the general patterns that are present in other published works (Wallinga *et al.* 2006). Incorporating these changes to transmission into the traditional SEIR compartmental model now gives us equations (3a), (3b), (3c) and (3d)

$$\dot{S}_\alpha = -\beta S_\alpha \left(\sum_{i=1}^{4} C(\alpha, i) I_i \right) - v_\alpha \tag{3a}$$

$$\dot{E}_\alpha = \beta S_\alpha \left(\sum_{i=1}^{4} C(\alpha, i) I_i \right) - \delta E_\alpha \tag{3b}$$

$$\dot{I}_\alpha = \delta E_\alpha - \gamma I_\alpha \tag{3c}$$

$$\dot{R}_\alpha = \gamma I_\alpha + v_\alpha \tag{3d}$$

where α represents the age group (0-4, 5-19, 20-39, 40+). The parameter δ is the rate (per day) at which individuals moved from the exposed to infectious classes. The inverse of δ is the mean time an individual spends in the exposed class before transitioning to the infectious class. γ is the rate (per day) at which individuals leave the infectious class i.e., recover from infection. The inverse of γ is the mean time an individual spends in the infected class before transitioning to the recovered class. In the susceptible and removed equations, v_α is a vaccination function the specific age group α. The function takes its values from the numbers of people vaccinated in each age group as reported by the Direction de Santé Publique de Montreal (DSP). It's derivation is shown in equation (4).

Vaccination

Studies have used 14 days for the period between vaccination and protection (Baguelin *et al.* 2010). It is unknown what happens if someone is infected after they receive a vaccination but before they receive full immunity from the vaccine. Efficacy of the vaccine has been estimated as being as high as 70% to 98% (Greenberg *et al.* 2009, Clark *et al.* 2009, GlaxoSmithKline Canada 2009).

When vaccination in Montreal started on calendar week 42 (October 24, 2009) of the pandemic, a proportion, described by equation (4), of individuals in the susceptible compartment of the model were removed and placed into the Recovered compartment.

Fourteen days after the vaccination date, a proportion of individuals would be removed from the susceptible category with 100% efficacy. Individuals do not gradually develop protection from infection as is done in Milne *et al.* (2009), they go from being completely susceptible to completely protected. As the susceptible category becomes smaller relative to the initial population size, the vaccination effectiveness decreases. This accounts for the chance a vaccinated individual becomes infected before the 14 day period.

$$v_\alpha(t) = V_\alpha(t-\tau)\frac{S_\alpha(t)}{N_\alpha} \tag{4}$$

where τ is the 14 day delay before immunity and V_α is the weekly vaccination data by age group.

Parameter Estimation

For our model we fixed the latent period $1/\delta$=2.62 days and the infectious period $1/\gamma$ =2.00 days (Tuite *et al.* 2010). For the contact matrix we set b=0.4a and c_1=c_3=4a. For our initial conditions, S_α, E_α and I_α, we used census data from Statistics Canada (Institut de la statistique Quebec 2006) and estimated the initial number of infected and exposed individuals in each age group by fitting our model to data. To account for the underreporting of confirmed cases we estimated age specific reporting ratios, ε_α, as well as a separate reporting ratio for the second wave, *W2*, which we hypothesize to have a larger degree of underreporting then the first wave. To estimate these parameters we found the most likely reporting ratios, ε_α, for each specific age group. These reporting ratios tell us how many cases a single predicted case from our model represents. We

simplified the search for the estimated number of initial *Exposed* and initial *Infectious* people by solving for a single parameter. This single parameter, x, is the sum of initial exposed and initial infected individuals across all ages. The parameter was then split between the initial *Exposed* and *Infectious* class proportional to the time a typical individual spends in those classes. The *Exposed* and *Infectious* totals were then proportionally distributed across the different age classes.

To estimate the unknown parameter values we found maximum likelihood estimates based on a Poisson distribution of observed cases. This involved the optimization function *fminsearch* in Matlab, a computing program used for creating functions and simulations. *Fminsearch* uses a Nelder-Mead simplex algorithm to minimize the Poisson negative log likelihood function and solve for the most likely parameter values simultaneously (eight values in total). We simultaneously fit our model to four sets of data, the confirmed weekly cases for 0-4 year olds, 5-19 year olds, 20-30 year olds and 40+ year olds. Our simulation creates age specific incidence time series using the vaccination, AH, contact matrix and school timing data. The model estimates the number of cases for each age group over the entire course of the epidemic as well as the parameters a and the initial numbers of exposed and infectious individuals at the start of the epidemic. These steps are repeated until the maximum likelihood values are found for each of the parameters.

Parameter	Description	Value	Method
a	contacts within age groups	8.76×10^{-6}	Fit
$\varepsilon_{0\text{-}4}$	0-4 reporting ratio	3.01×10^{-2}	Fit
$\varepsilon_{5\text{-}19}$	5-19 reporting ratio	9.29×10^{-3}	Fit
$\varepsilon_{20\text{-}39}$	20-39 reporting ratio	1.30×10^{-2}	Fit
ε_{40+}	40+ reporting ratio	9.23×10^{-3}	Fit
$W2$	second wave reporting	0.183	Fit
y	Humidity resposne parameter	0.107	Fit
$E_{0\text{-}4}$	Initial Exposed age 0 to 4	0.315	Set
$E_{5\text{-}19}$	Initial Exposed age 5 to 19	0.974	Set
$E_{20\text{-}39}$	Initial Exposed age 20 to 39	1.87	Set
E_{40+}	Initial Exposed age 40+	2.32	Set
$I_{0\text{-}4}$	Initial Infectious age 0 to 4	0.240	Set
$I_{5\text{-}19}$	Initial Infectious age 5 to 19	0.743	Set
$I_{20\text{-}39}$	Initial Infectious age 20 to 39	1.43	Set
I_{40+}	Initial Infectious age 40+	1.77	Set

Table 1- Maximum likelihood estimates of the parameters obtained by fitting the model to the data. Set values were found by solving for the total initial infected then dividing proportionately by population size and duration of average time in each state.

Reproductive Value

the basic reproductive number of a disease R_0 is the average number of secondary cases produced by a typical infected individual during his/her entire period of infectiousness in a completely susceptible population. R_0 is an important metric for establishing whether or not there will be an epidemic. R_0 is the average number of secondary infections caused my one infectious individual in a homogeneously mixing, completely susceptible population. Values of $R_0<1$ will result in the disease dying out whereas values of $R_0>1$ there will result the spread of the disease in the populations and possibly an epidemic. The next generation method was used to calculate the reproductive

number and the effective reproductive number, R_{eff}, for our model (Diekmann *et al.* 1990). The effective reproductive number, R_{eff}, is the average number of secondary infections caused by one infectious individual in the current population. The two differ since R_{eff} takes into account the current size of the susceptible pool and R_0 initial size of the susceptible pool. R_0 and R_{eff} are defined as the dominant eigenvalue of a positive linear operator $K(S)$ (Diekmann *et al.* 1990). R_0 is calculated using the initial population size while R_{eff} is calculated with the population size at time t. $K(S)$ for our system of equations is defined as:

$$K(S) = \beta_t \times C_{ij} \times N_i \times D^{-1}$$

where D is a diagonal matrix with recovery rates of the different age classes on the diagonal, C_{ij} is the contact matrix, N_i is the susceptible population size of age group i and β_t is the vapour pressure coefficient on day t. Due to β_t, changing with the daily average absolute humidity and the transmission matrix changing with the school calendar, we calculate R_0 (Figure1) and R_{eff} (Figure 2) every day of the pandemic.

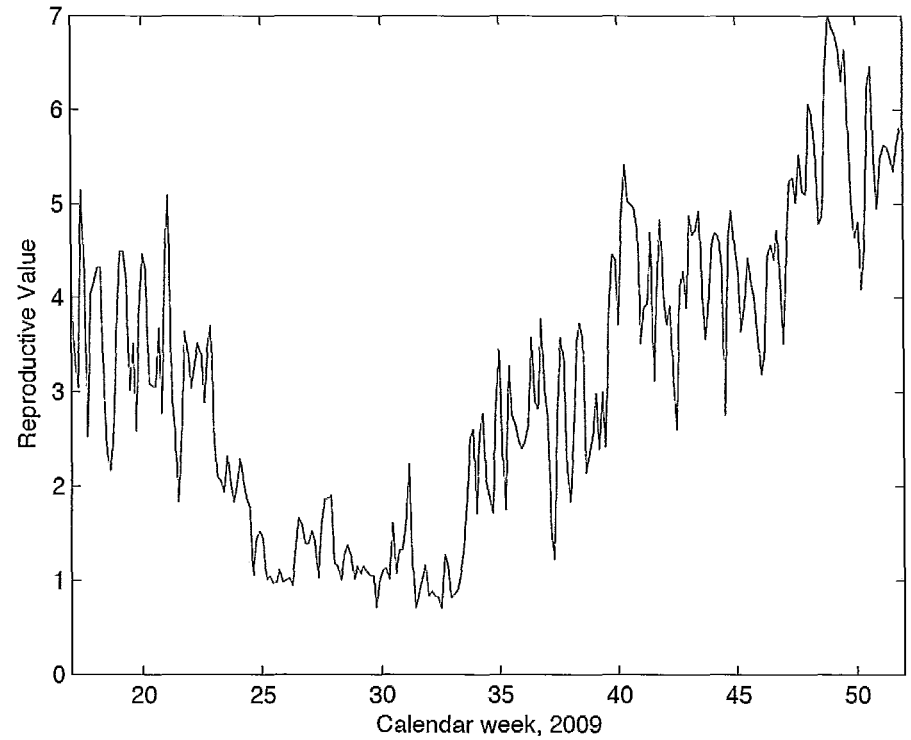
Reproductive Value
Calendar week, 2009
0
1
2
3
4
5
6
7
20
25
30
35
40
45
50

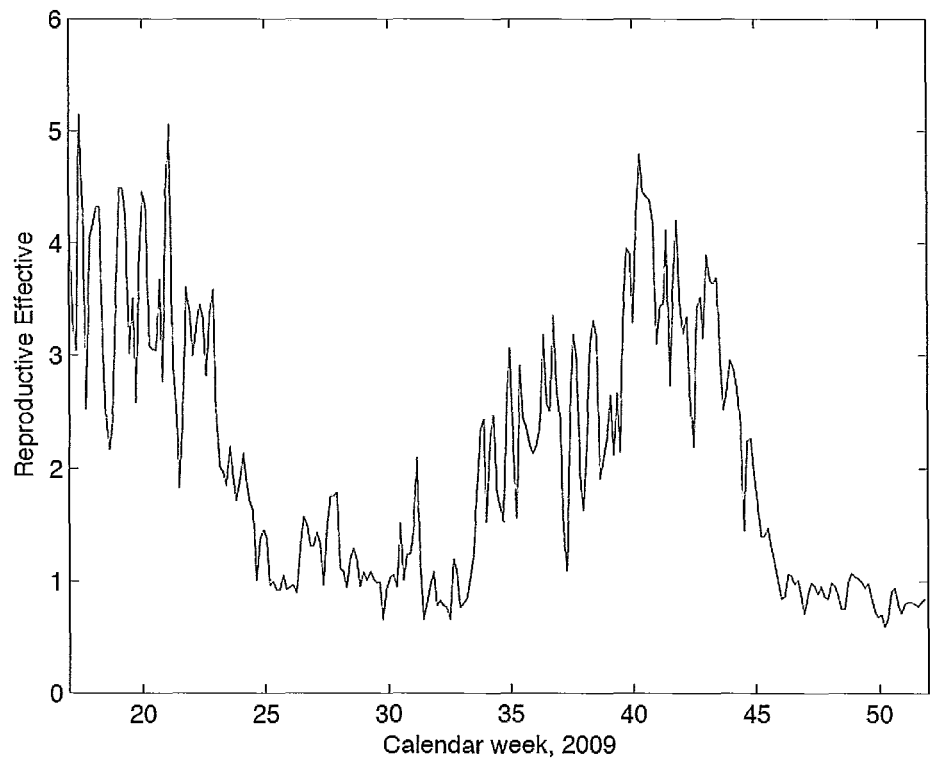
Reproductive Effective
Calendar week, 2009
0
1
2
3
4
5
6
20
25
30
35
40
45
50

Figures 1 and 2 - Top - R_0 plotted for the course of both pH1N1 incidence waves in Montreal. The calculation uses the initial susceptible pool size for the entire time period. Bottom - R_{eff} plotted for the course of both pH1N1 incidence waves in Montreal. The calculation allows for the size of the susceptible pool to change over the time period.

Model Simulations

After fitting our model to the data provided by the DSP we ran three simulations. We ran our model with and without school closures. Our first simulation of the pH1N1 pandemic in Montreal was with school closures during the summer holidays. The second simulation allowed school-aged children to remain in school throughout the summer holidays. The third simulation examines the impact a school closure has during the initial phases of the second wave. For the third simulation we examine what happens if the children do not return to school. Overdispersion was calculated for the model (value 5.54) but we did not use it to change our parameter estimates.

Results

The model differs from the observed data in several ways (Figures 3 to 8). The model gives a much higher number of cases for each wave than what were observed in the data (see reporting ratios in Table 1). This is not surprising due to the known levels of under-reporting of the true prevalence of cases. Also, the numbers of infected children aged 0-4 in the model is relatively lower (to the other age groups) than the reported cases. This may be due to a bias in reporting. If parents are more likely to get their children tested for pH1N1 than they are for themselves, this may lead to the relative under-

representation of adults in the data. In the first wave, the model overestimates the incidence in the two youngest age groups but underestimates the incidence in the older age groups. Also, the local peak in the incidence for school-aged children in week 19 was not recreated by the model. In the second wave, the model slightly overestimates the number of 20-39 year-olds that were infected. In general, the timing of the incidence peaks is in line with the data from the DSP.

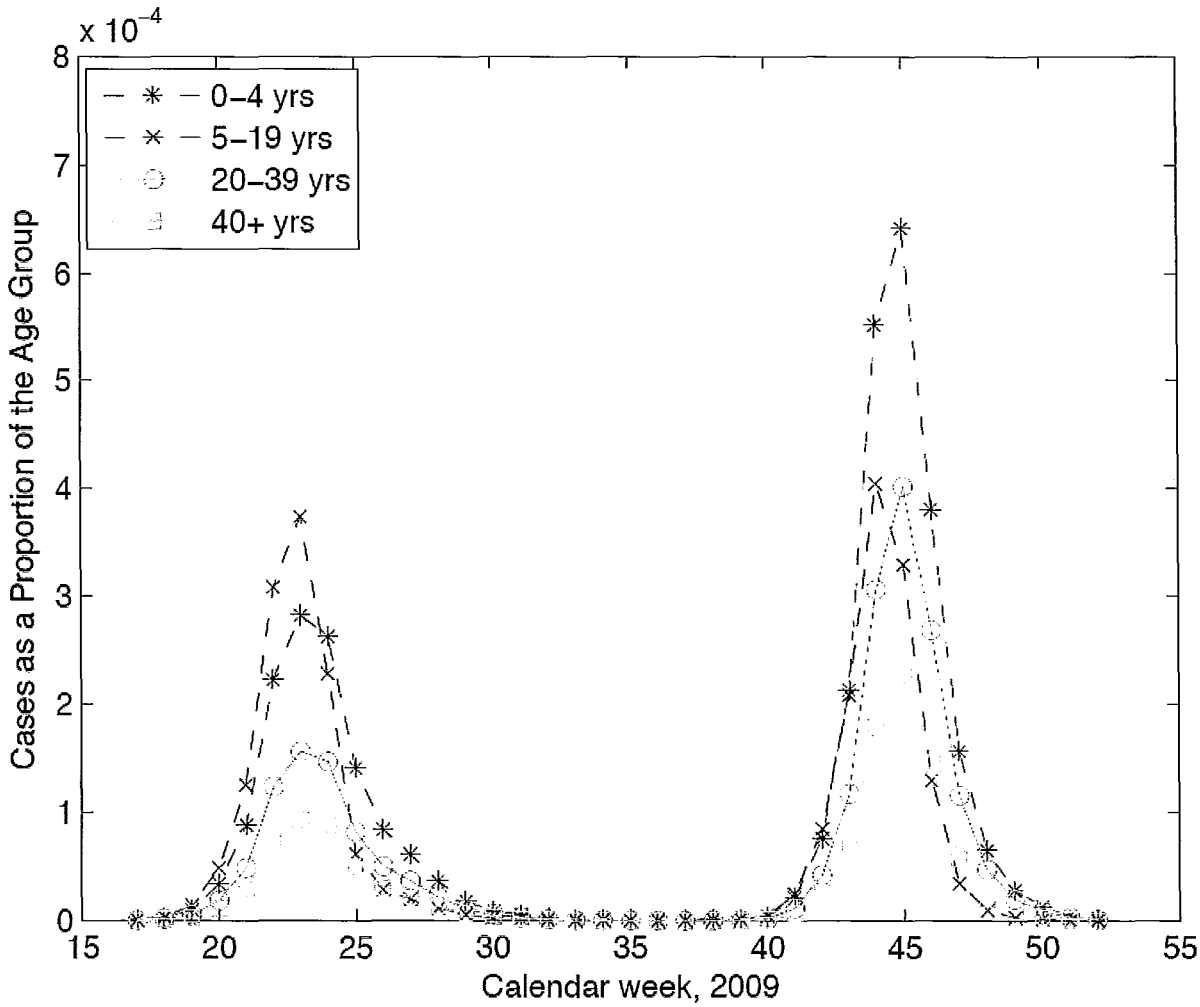

Figure 3 - Model prediction for the spring and fall waves of the 2009 pandemic.

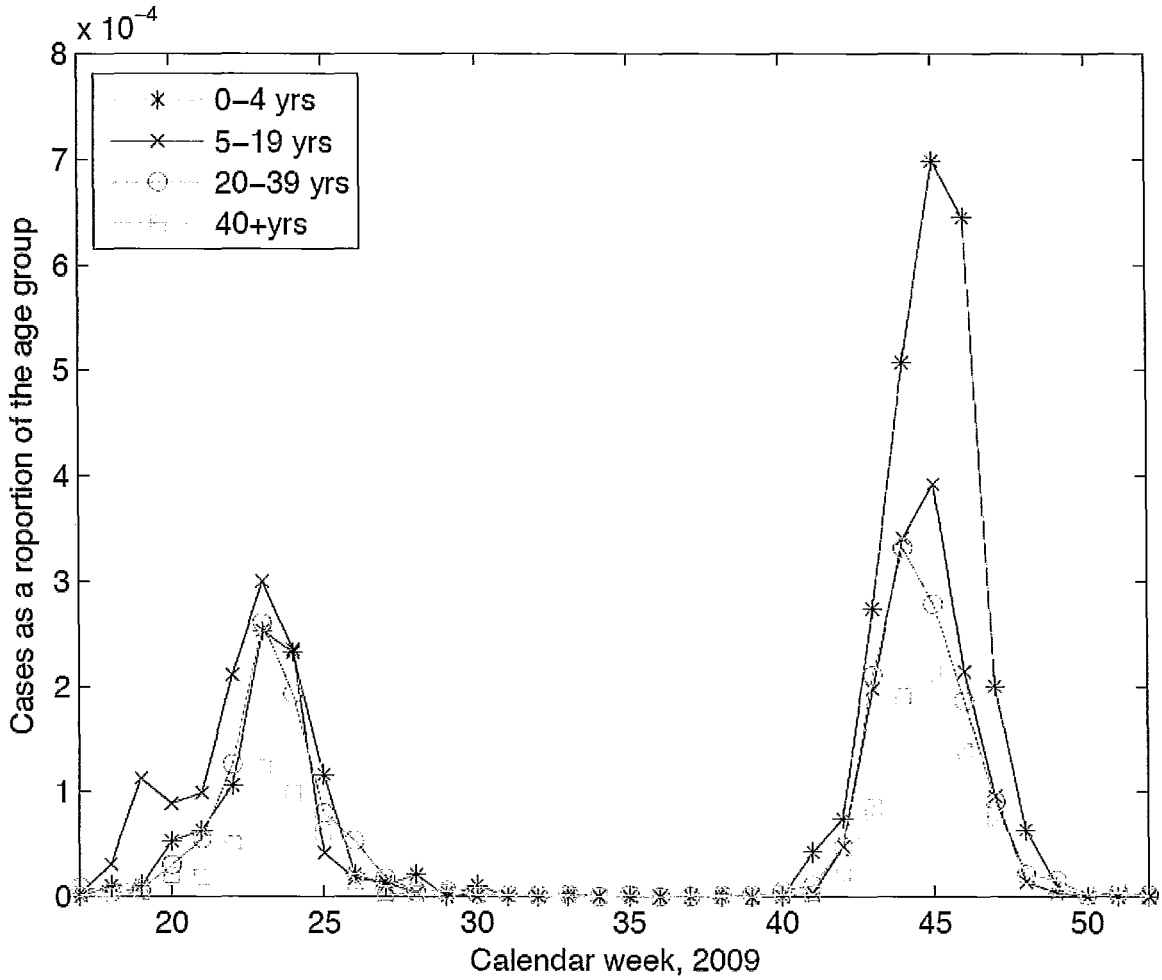

Figure 4 - Laboratory confirmed cases of pH1N1 as a proportion of the age group plotted over the course of both incidence waves.

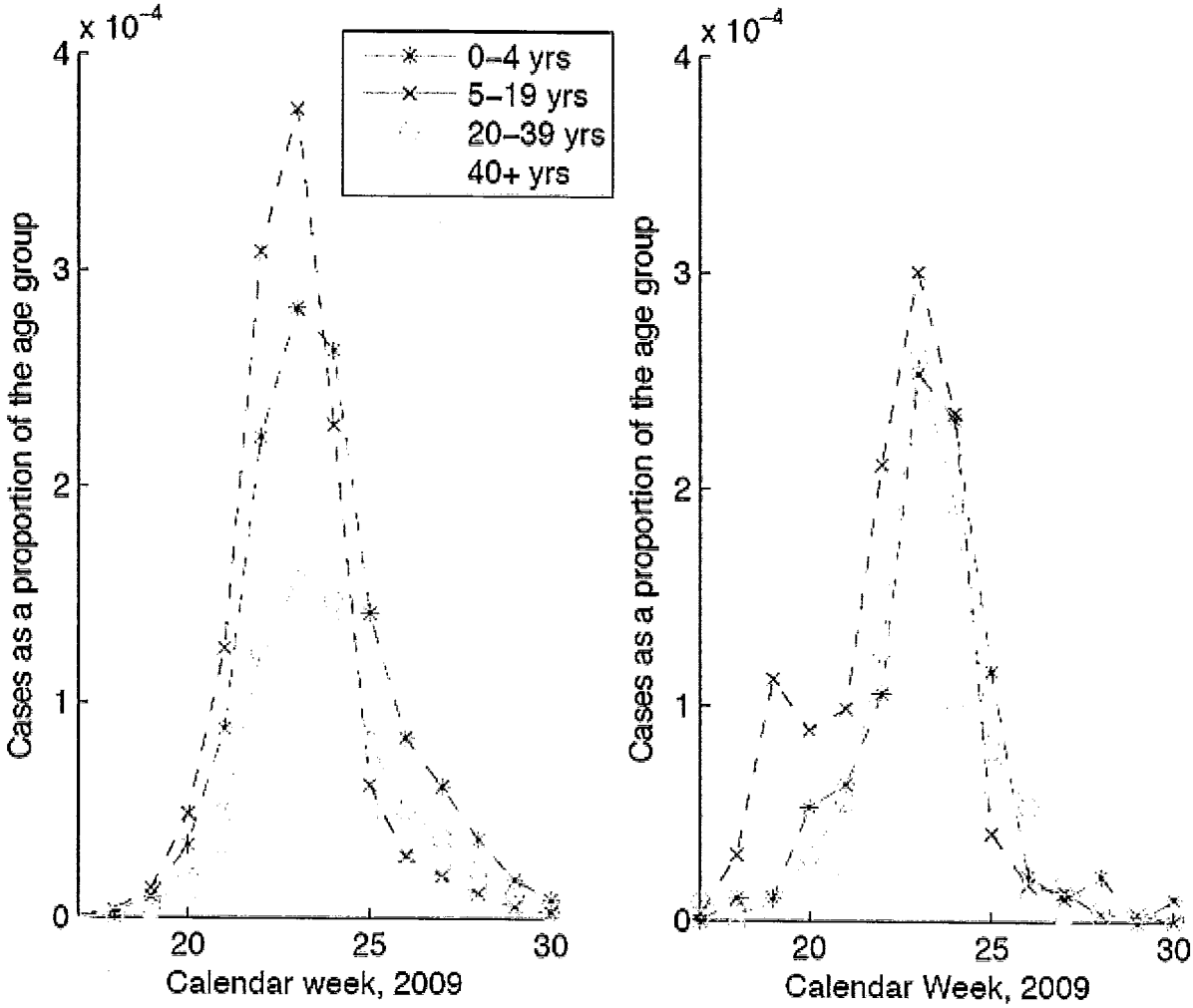

Figure 5 - Left: model prediction for the first wave of the pandemic, sorted by age group. Right: Laboratory confirmed cases of pH1N1 infection from the DSP for the first incidence wave, sorted by age group.

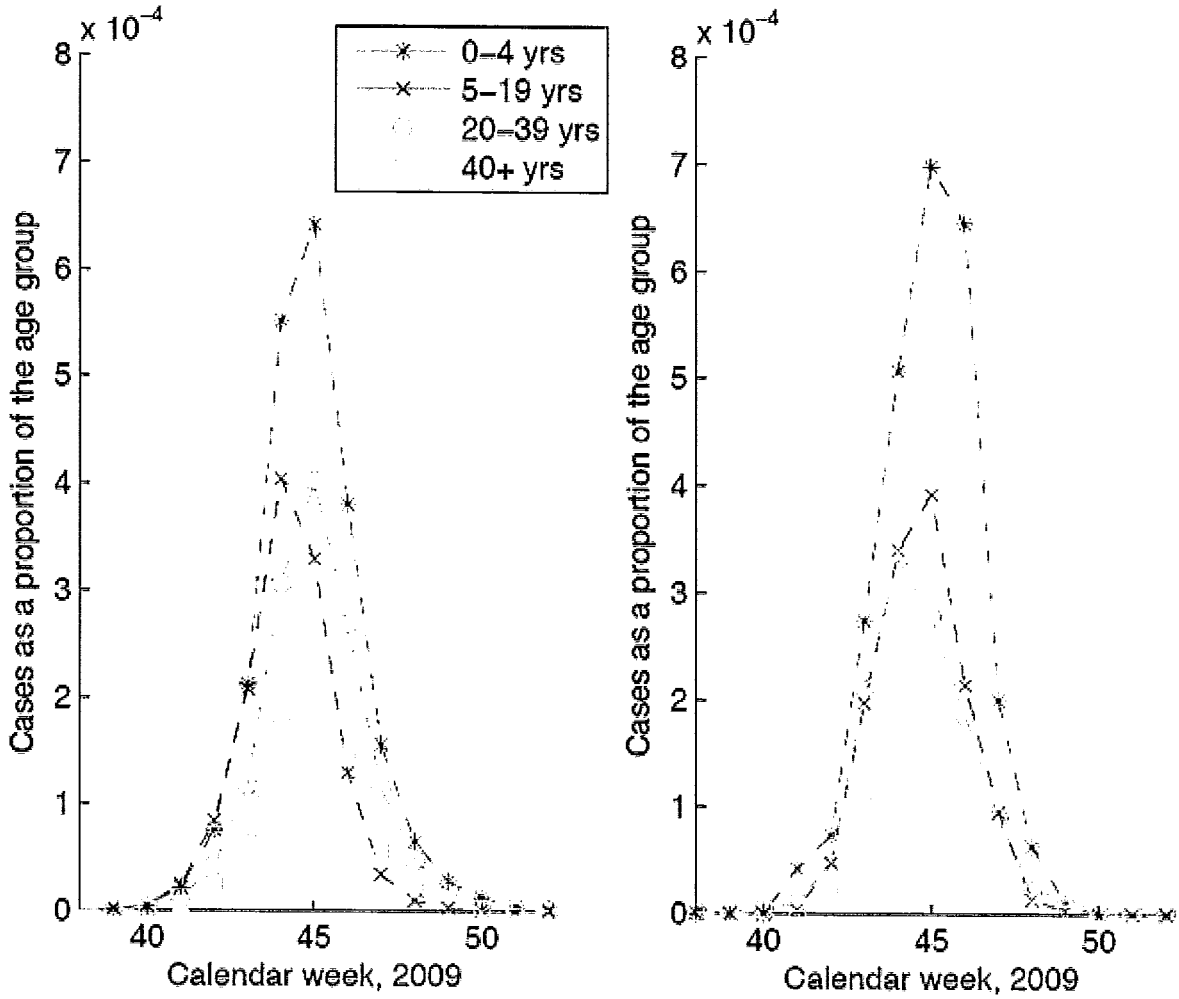

Figure 6 - Left: model prediction for the second wave of the pandemic, sorted by age group. Right: Laboratory confirmed cases of pH1N1 infection from the DSP for the second incidence wave, sorted by age group.

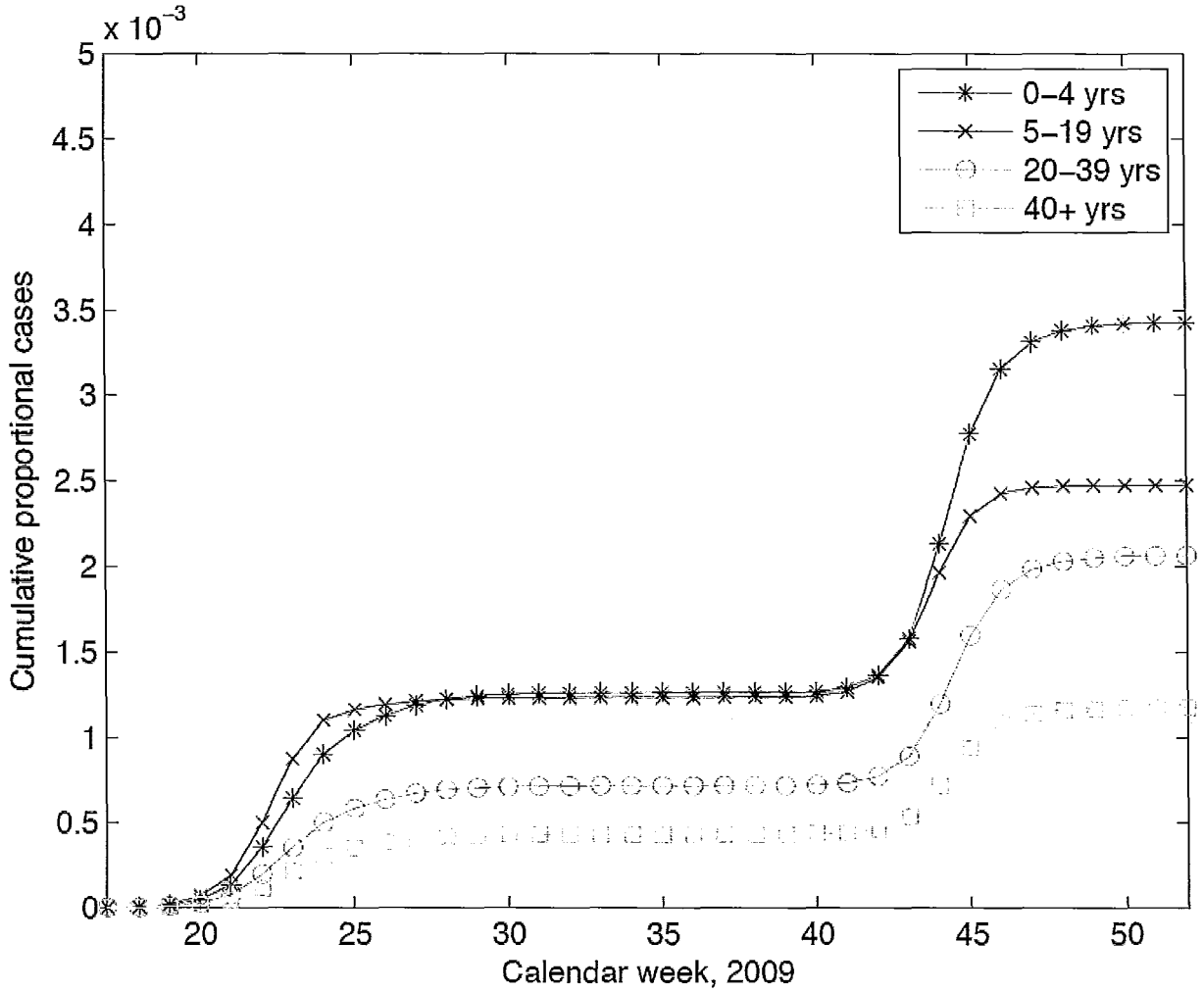

Figure 7 - Cumulative cases predicted from the model as a proportion of age group.

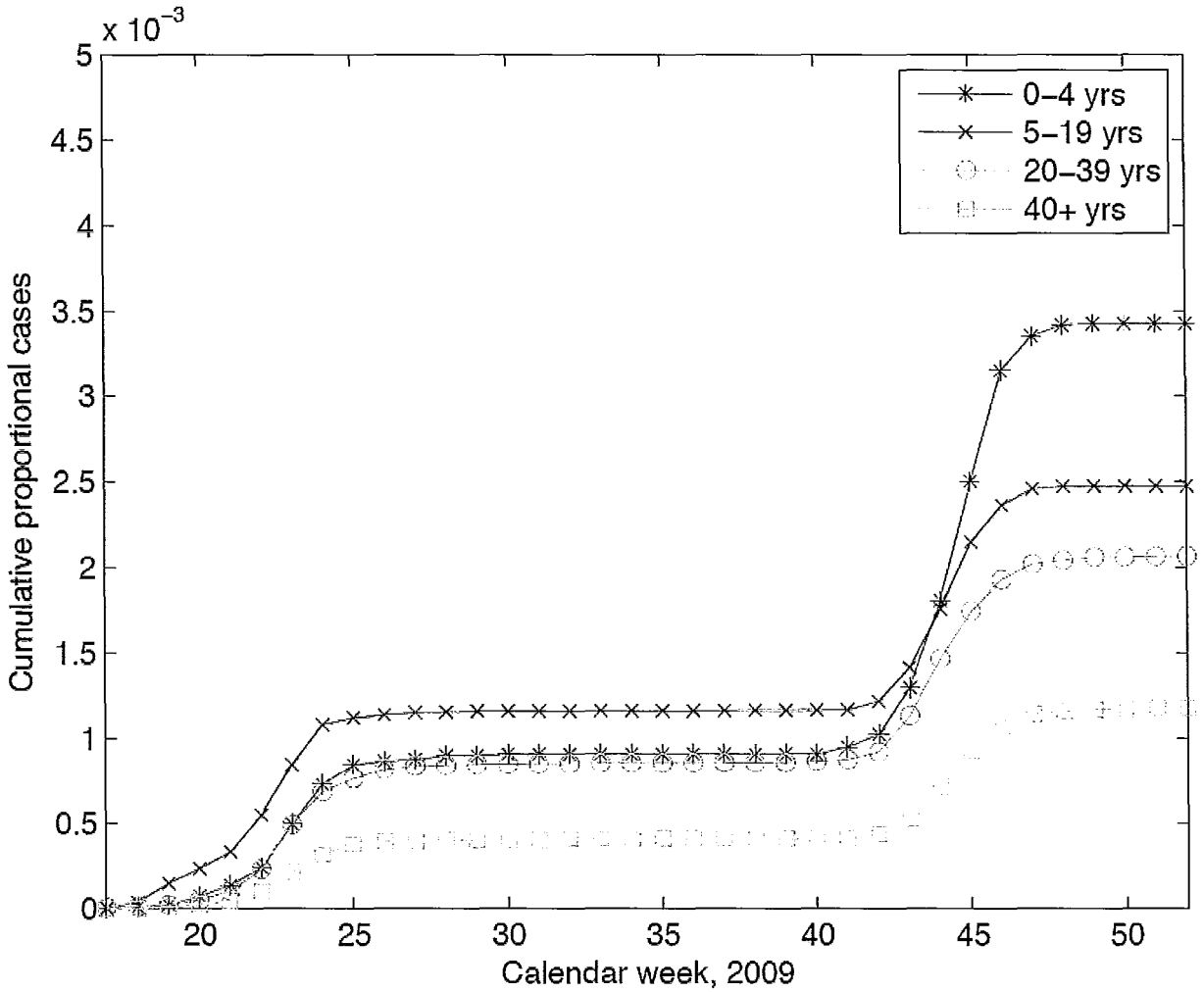

Figure 8 - Laboratory confirmed cases plotted cumulatively as a proportion of age group.

Effects of School Closures

We modeled the effects of continuous school (Figures 9 and 10). To do this we let the contact behaviour of school-aged children with individuals of their own age group remain the same throughout the year, where previously we decreased school-aged contacts during the summer holidays. We also simulated extended school closures, in which children do not return to school in the Fall semester (Figures 11 and 12). During

one of our standard simulations, with reduced school-aged contacts during the summer holidays, our model predicts the same number of total confirmed cases at the end of December 2009 as the collected surveillance data (324 0-4 cases, 726 5-19 cases, 1164 20-39 cases and 1066 40+ cases). When we simulate school-aged children not returning to school in the Fall, the total number of cases reduces to, 213 0-4 cases, 482 5-19 cases, 867 20-39 cases and 743 40+ cases at the end of December 2009 (Figures 11 and 12). This gives us a total of 975 cases across all age groups averted through children not returning to school for the Fall semester.

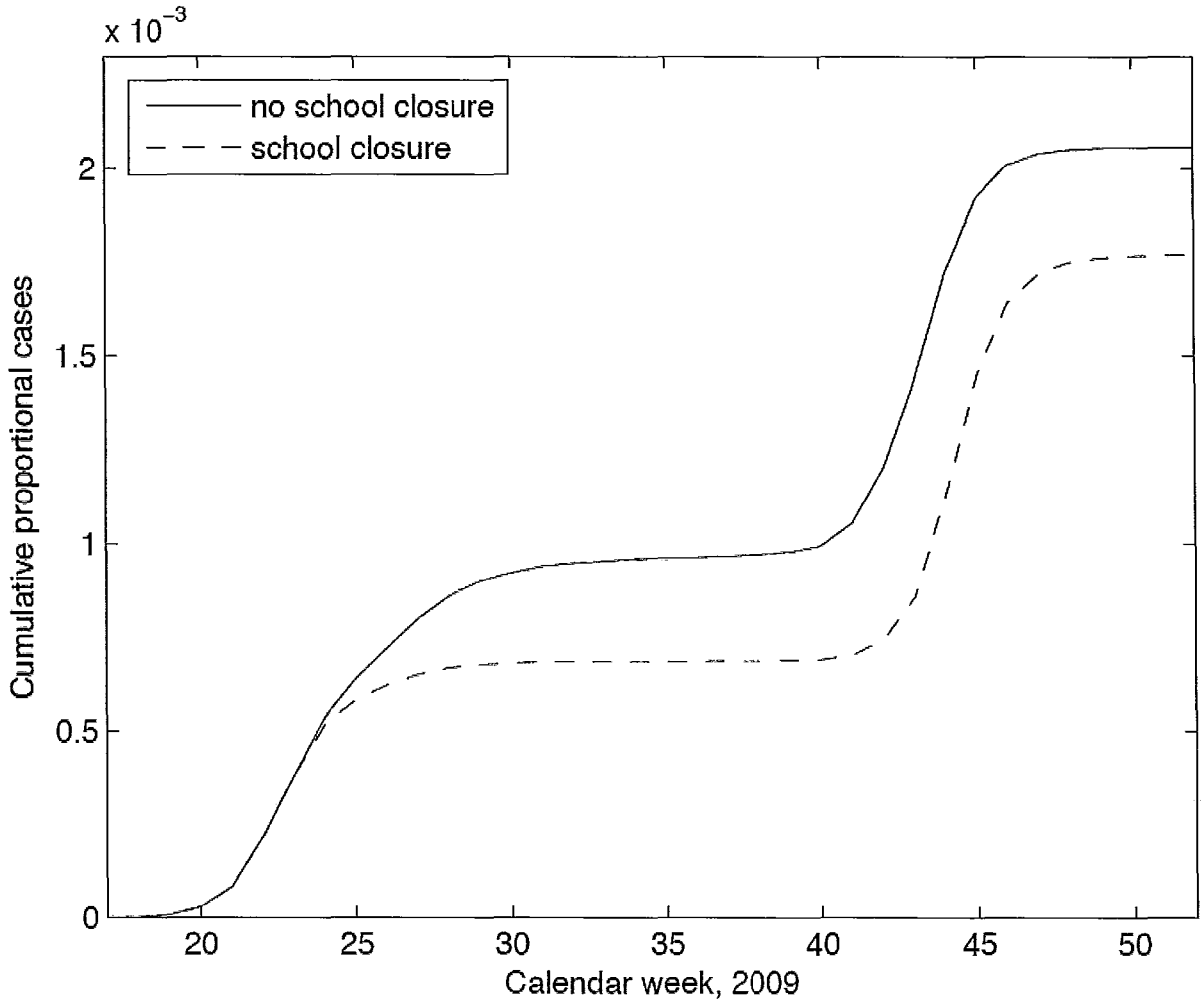

Figure 9 - Cumulative cases predicted by the model with schools not closing in the summer. The solid line is for continuous school and the dashed line is with school closure.

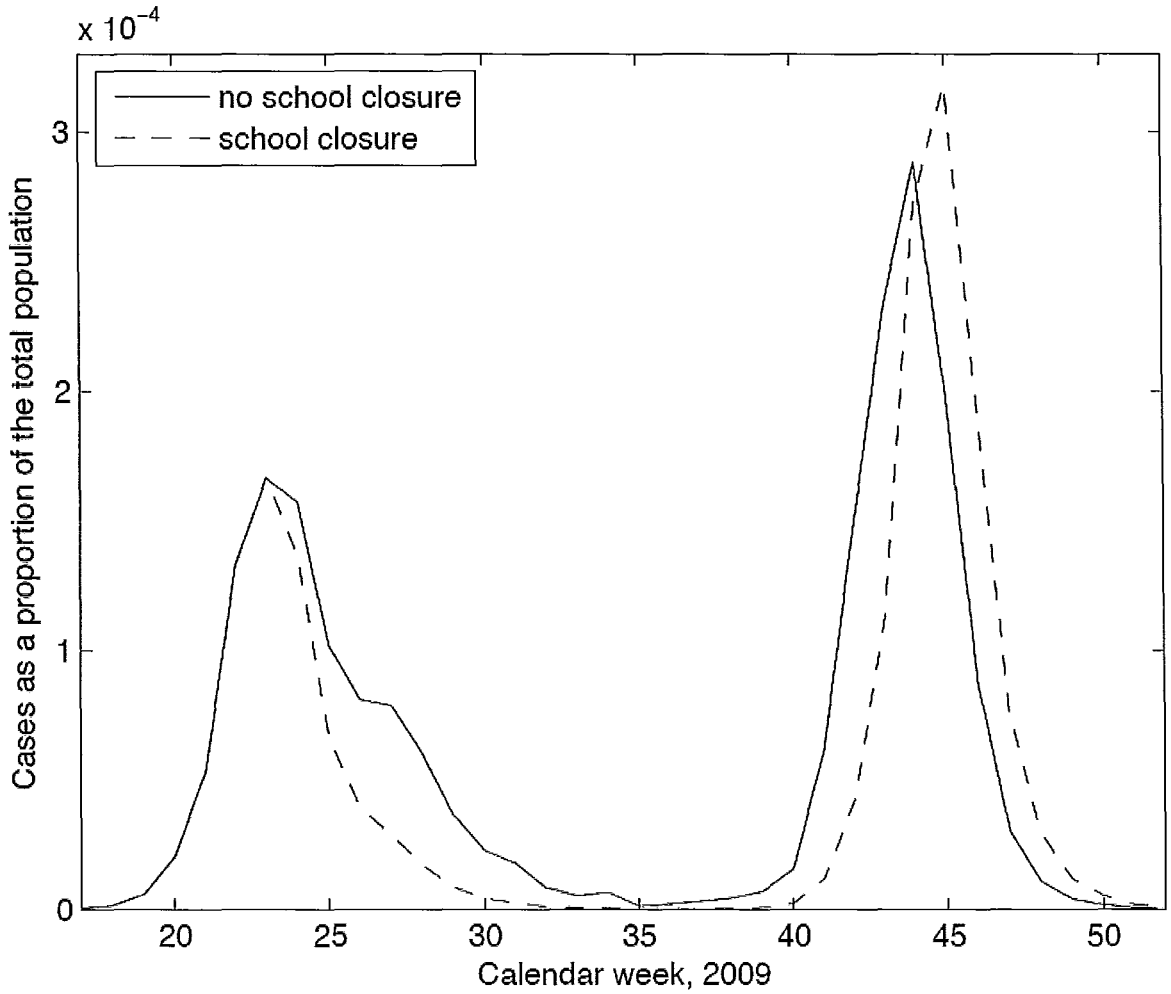

Figure 10 - Incident cases as a proportion of the total population predicted by the model with schools not closing in the summer. The solid line is for continuous school and the dashed line is with school closure.

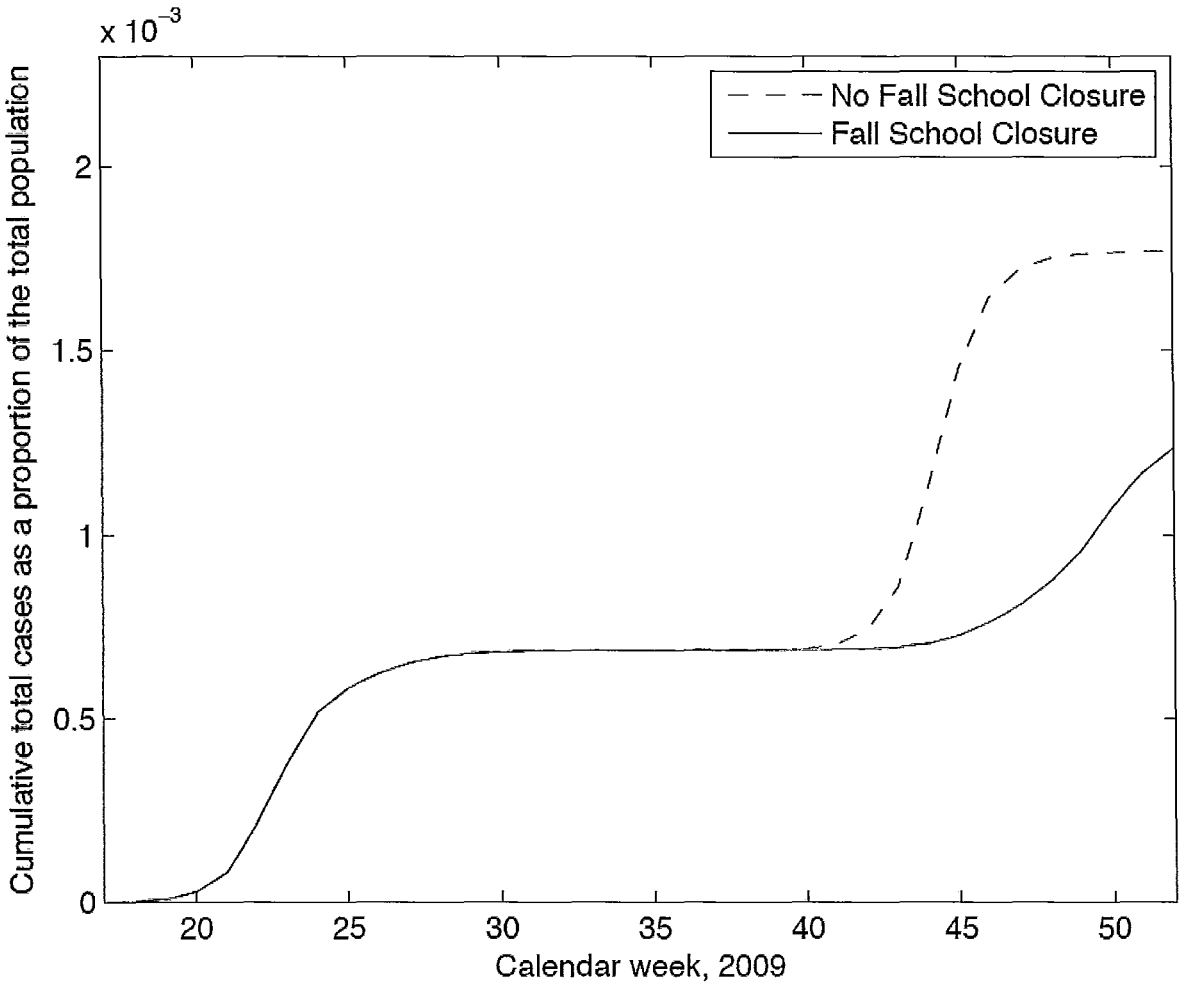

Figure 11 - Cumulative cases as a proportion of the total population. The solid line is for the model run with school closure for 5-19 year olds. The dashed line is with a Fall semester school closures (children do not return to school for the Fall semester).

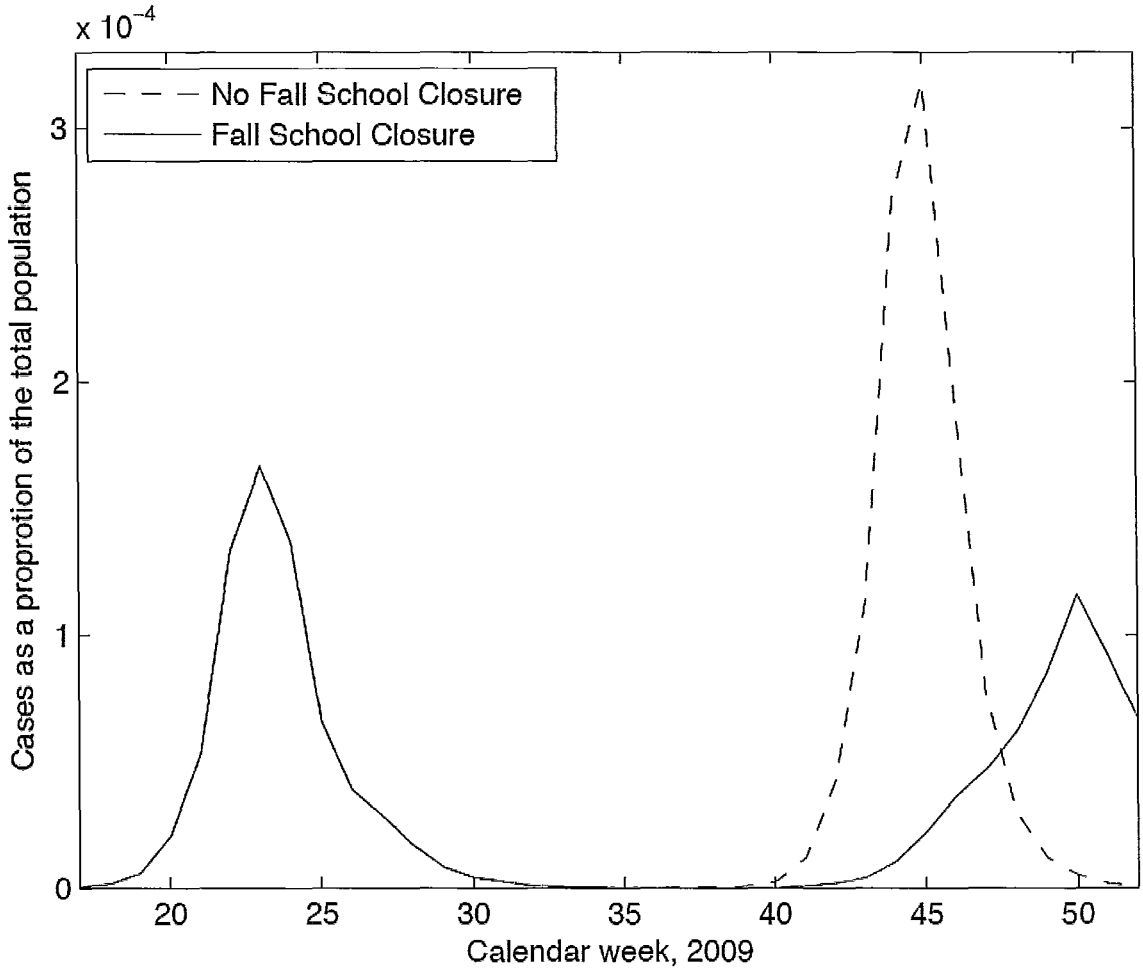

Figure 12 - Incident cases as a proportion of the total population: In solid is the model simulation for 5-19 year olds having summer holidays then return to school in the fall. The dashed line is a simulation where children do not return to school after summer vacation.

Discussion

In this study we have modeled the 2009/2010 influenza pandemic in Montreal and shown that the combination of changing contact rates for children as well as accounting for variation in absolute humidity can reproduce the two waves.

For the first wave of the pandemic to stop there must have been a reduction in R_{eff}. This would most likely be due to the depletion of susceptible individuals and/or a decrease in the transmission rate. In this paper we show that with two assumptions about influenza virus transmission we are able to model both waves of the pandemic with one model, and without depleting the majority of the susceptible pool until the end of the pandemic. The decline in average daily contacts between school-age children during the summer holidays is a strong enough factor to create two waves but triggers the start of the second wave too prematurely. The additional impact of seasonality, in the form of absolute humidity, generated multiple waves at the appropriate time.

We found reporting ratios for the different age groups by comparing the surveillance data to the model results (see Table 1). We believe that the surveillance is an underestimate of the number of true cases in the population and the reporting ratios allow us to quantify the difference. Our model predicts that during the second wave, the level of underreporting was about five times more than in the first wave. We also find that the group with the least underreporting is the 0-4 age group. This is not surprising, since parents are more likely to take their sick child to a clinic before they take themselves. One of the challenges of recreating the disease outbreak is the uncertainty in the actual level of disease in the population. Over the months of the pH1N1 outbreak, health officials changed the message to citizens and doctors. Sometimes the message was to go to a doctor and get tested, other times the message was to self-isolate unless the person felt very ill or had severe symptoms. There is also a concern about the adherence to official

testing policy that was done at hospitals and doctors' offices. All of these factors mean that there is uncertainty in the level of underreporting of pH1N1 cases.

The model predicts the incidence of disease in different age classes throughout the epidemic by comparing the simulation results to the reported incidence values. The people age 5-19 and 40+ have the lowest reporting efficiency values. By comparing the model's predictions and the vaccination counts one can conclude that the depletion of school-age susceptible people contributed significantly to the ending of the pandemic. Approximately 60% of the school-aged children were vaccinated and the model predicts that approximately 27% of the group became infected at some point during the epidemic. This leaves very few people aged 5 to 19 to spread the virus and sustain high levels of transmission.

The difference between the reported number of incident cases and the actual prevalence has been estimated as 79 times (90% CI 47-148) (Reed *et al.* 2009) and 100 times (Sander *et al.* 2009). We found that incidence values may be off by a factor of 33 to 108 (1/reporting ratio) for our different age groups during the initial wave and approximately five times that for the second wave. We note that improved methods for dealing with uncertainty in surveillance would be useful. This may involve combining traditional surveillance methods along with online surveys, phone call volume to medical help lines and school absenteeism data may be used to generate better estimates of disease incidence. Google Flu Trends is a novel tool that may be used towards the goal of improved disease surveillance.

It was predicted that the reduction in cases among school-age individuals would be greater than that observed in typical seasonal influenza seasons based on early surveillance data (Cauchemez *et al.* 2009). In total, over 15% of cases may be averted through school closure based on studies of previous influenza epidemics (Cauchemez *et al.* 2009). Our findings on the relation between school closure and humidity on incidence may lead to future studies of timing of school closure.

Literature Cited

Baguelin, M., Van Hoek, A. J., Jit, M., Flasche, S., White, P. J. & Edmunds, W. J. (2010) Vaccination against pandemic influenza A/H1N1v in England: A real-time economic evaluation. *Vaccine* **28**:2370-2384.

Bjørnstad, O. N., Finkenstädt, B. F. & Grenfell, B. T. (2002) Dynamics of Measles Epidemics: Estimating Scaling of Transmission Rates Using a Time Series SIR Model. *Ecological Monographs* **17**(2):169-184.

Cannell, J. J., Zasloff, M., Garland, C. F., Scragg, R. & Giovannucci, E. (2008) On the Epidemiology of Influenza. *Virology Journal* **5**:29.

Cauchemez, S., Donnelly, C. A., Reed, C., Ghani, A. C., Fraser, C., Kent,C. K., Finelli, L. & Ferguson, N. M. (2009) Household Transmission of 2009 Pandemic Influenza A (H1N1) Virus in the United States. *The New England Journal of Medicine* **361**: 2619-2627.

Chowell, G., Ammonb, C. E., Hengartnera, N. W. & Hymana, J. M. (2006) Transmission dynamics of the great influenza pandemic of 1918 in Geneva, Switzerland: Assessing the effects of hypothetical interventions. *Journal of Theoretical Biology* **241**: 193-204.

Clark, T. W., Pareek, M., Hoschler, K., Dillon, H., Nicholson, K.G., Groth, N. & Stephenson, I. (2009) Trial of 2009 influenza A (H1N1) monovalent MF59-adjuvanted vaccine. *The New England Journal of Medicine* **361**(25): 2424-2435.

Diekmann, O., Heesterbeek, J. A. P. & Mets, J. A. J. (1990) On the definition and the computation of the basic reproductive ratio in models for infectious diseases in heterogeneous populations. *Journal of Mathematical Biology* **28**: 365-382.

Dushoff, J., Plotkin, J. B., Levin, S. A. & Earn, D. J. D. (2004) Dynamical resonance can account for seasonality of influenza epidemics. *Proceedings of the National Academy of Sciences of the United States of America* **101**:16915-16916.

Ferguson, N. M., Cummings, D. A. T., Fraser, C., Cajka, J. C., Cooley, P. C. & Burke, D. S. (2006) Strategies for mitigating an influenza pandemic. *Nature* **442**: 448-452.

Fisman, D. N., Savage, R., Gubbay, J., Achonu, C., Akwar, H., Farrell, D. J., Crowcroft, N. S. & Jackson, P. (2009) Older Age and a Reduced Likelihood of 2009 H1N1 Virus Infection. *The New England Journal of Medicine* **361**: 2000-2001.

GlaxoSmithKline Canada. Arepanrix H1N1AS03-Adjuvanted H1N1 pandemic influenza vaccine. Product information leaflet. (2009) Available at: http://www.hc-

sc.gc.ca/dhp-mps/prodpharma/legislation/interimorders-arretesurgence/prodinfo-vaccin-eng.php

Greenberg, M. E., Lai, M. H., Hartel, G. F., Wichems, C.H., Gittleson, C., Bennet, J., Dawson, G., Hu, W., Leggio, C., Washington, D. & Basser, R.L. (2009) Response after one dose of a monovalent 2009 influenza A (H1N1). *The New England Journal of Medicine* **361**: 2405-2413.

Hancock, K., Veguilla, V., Lu, X., Zhong, W., Butler, E. N., Sun, H., Liu, F., Dong, L., DeVos, J. R., Gargiullo, P. M., Brammer, T. L., Cox, N. J., Tumpey, T. M. & Katz, J. M. (2009) Cross-Reactive Antibody Responses to the 2009 Pandemic H1N1 Influenza Virus. *The New England Journal of Medicine* **361**:1945-1952.

Institut de la statistique Quebec. Population by age group, Montreal and Laval administrative regions, 2006 Statistics Canada, 2006 Census of Canada. Accessed March 3, 2009.

Lipsitch, M. & Viboud, C. C. (2009) Influenza seasonality: lifting the fog. *Proceedings of the National Academy of Sciences of the United States of America* **106**(10): 3645-3646.

Longini, I. M. Jr., Koopman, J. S., Monto, A. S., Fox, J. P. (1982) Estimating household and community transmission parameters for influenza. *American Journal of Epidemiology* **115**: 736-751.

Lowen, A. C., Mubareka, S., Steel, J. & Palese, P. (2007) Influenza Virus Transmission Is Dependent on Relative Humidity and Temperature. *PLoS Pathogens* **3**: 1470-1476.

Lunelli, A., Pugliese, A. & Rizzo, C.: Epidemic patch models applied to pandemic influenza (2009) Contact matrix, stochasticity, robustness of predictions. *Math Bioscience* **220**: 24-33.

Medlock J., Galvani AP (2009) Optimizing Influenza Vaccine Distribution. *Science* **325**: 1705-1708.

Medlock J., Meyers, L. A., & Galvani, A. Optimizing allocation for a delayed influenza vaccination campaign. Version 2. PLoS Currents Influenza. 2009 December 11 [revised 2010 January 29]: RRN1134.

Metzger, K. B., Hajat, A., Crawford, M. & Mostashari, F. (2004) How Many Illnesses Does One Emergency Department Visit Represent? Using a Population-Based Telephone Survey to Estimate the Syndromic Multiplier. *MMWR Morbidity and Mortality Weekly Report* **53**: 106-111.

Miller, E., Hoschler, K., Hardelid, P., Stanford, E., Andrews, N. & Zambon, M. (2010) Incidence of 2009 pandemic influenza A H1N1 infection in England: a cross-sectional serological study. *Lancet* **375**(9720):1100-1108.

Miller, M. A., Viboud, C., Balinska, M. & Simonsen, L. (2009) The Signature Features of Influenza Pandemics - Implications for Policy. *The New England Journal of Medicine* **360**: 2595-2598.

Milne, G., Kelso, J. & Heath, K. (2009) Strategies for mitigating an influenza pandemic with pre-pandemic H5N1 vaccines. *Journal of the Royal Society Interface* 7:573-586.

Mossong, J., Hens, N., Jit, M., Beutels, P., Auranen, K., Mikolajczyk, R., Massari, M., Salmaso, S., Tomba, G. S., Wallinga. J., Heijne, J., Sadkowska-Todys, M., Rosinska, M. & Edmunds, W. J. (2008) Social Contacts and Mixing Patterns Relevant to the Spread of Infectious Diseases. *PLoS Medicine* **5**: 0381-0391.

Mylius, S. D., Hagenaars, T. J, Lugner, A. K. & Wallinga, J. (2007) Optimal allocation of pandemic influenza vaccine depends on age, risk and timing. *Vaccine* **26**: 3742-3749.

Nelson, W. A., Population Dynamics Statistical Methods. In: S.E. Jorgensen and B.D. Fath (eds), Population Dynamics. (2000) *Vol 4 of Encyclopaedia of Ecology*: 3350-3362. Elsevier.

Reed, C., Angulo, F. J., Swerdlow, D. L., Lipsitch, M., Meltzer, M. I., Jernigan, D. & Finelli, L. (2009) Estimates of the prevalence of pandemic (H1N1) 2009, United States, April-July 2009. *Emerging Infectious Diseases* **15**(12):2004-7.

Reid, A. H., Taubenberger, J. K. & Fanning, T. G. (2001) The 1918 Spanish influenza: integrating history and biology. *Microbes and Infection* **3**: 81-87.

Sander, B., Bauch, C., Fisman, D. N., Fowler, R., Kwong, J. C., McGeer, A., Zivkovic, G. M. & Krahn, M. (2009) Is a Mass Immunization Program for Pandemic (H1N1) 2009 Good Value for Money? Early Evidence from the Canadian Experience. *PLoS Currents Influenza* 2009 Dec 17:RRN1137.

Shaman, J. & Kohn, M. (2009) Absolute humidity modulates influenza survival, transmission, and seasonality. *Proceedings of the National Academy of Sciences of the United States of America* **106**(9):3243-8.

Shaman, J., Pitzer, V. E., Viboud, C., Grenfell, B. T. & Lipsitch, M. (2010) Absolute Humidity and the Seasonal Onset of Influenza in the Continental United States. *PLoS Biology* **8**(2): e1000316. doi:10.1371/journal.pbio.1000316.

Skwronski, D. M., De Serres, G., Crowcroft, N. S., Janjua, N. Z., Boulianne N., Hottes, T. S., Rosella, L. C., Dickinson, J. A., Rodica, G., Sethi, P., Ouhoummane, N., Willison, D. J., Rouleau, I., Petric, M., Fonseca, K., Drews, S. J., Rebbapragada, A., Charest, H., Hamelin, M., Boivin, G., Gardy, J. L., Li, Y., Kwindt, T. L., Patrick, D. M., Brunham R. C. and for the Canadian SAVOIR Team. (2010) Association between the 2008–09 Seasonal Influenza Vaccine and Pandemic H1N1 Illness during Spring– Summer 2009: Four Observational Studies from Canada. *Public Library of Science Medicine* 7(4): e1000258. doi:10.1371/journal.pmed.1000258.

Tuite, A. R., Greer, A. L., Whelan, M., Winter, A. L., Lee, B., Yan, P., Wu, J., Moghadas, S., Buckeridge, D., Pourbohloul, B. & Fisman, D. F. (2010) Estimated epidemiologic parameters and morbidity associated with pandemic H1N1 influenza. *Canadian Medical Association Journal* **182**(2):131-136.

Wallinga, J., Teunis, P. & Kretzschmar, M. (2006) Using Data on Social Contacts to Estimate Age-specific Transmission Parameters for Respiratory-spread Infectious Agents. *American Journal of Epidemiology* **164**: 936-944.

Conclusion

The research in this thesis focused on the 2009/2010 pandemic H1N1 outbreak in Montreal, Quebec, Canada. Research was conducted on the effectiveness of the vaccination campaign as well as on the factors contributing to the multi-wave structure. This research produced estimates of hospitalizations and deaths averted through the vaccination campaign. It also produced a model that incorporates age structure and environmental humidity that reproduces the disease incidence patterns observed in Montreal.

Chapter 1

In Chapter 1 a mathematical model was constructed and calibrated so that it could reproduce the pH1N1 incidence counts observed in Montreal, Quebec. The model incorporated the population size of Montreal, the idea that some people had pre-existing immunity to the virus and the numbers and timing of vaccinations administered. The model was then run with no one receiving a pH1N1 vaccination and the results were compared to the actual surveillance data. It was found that the vaccination campaign was associated with the prevention of between 320 and 1,553 hospitalizations and 4 and 19 deaths.

Chapter 2

In Chapter 2 a mathematical model was constructed with the goal of investigating the contribution of changing contacts and environmental humidity on the 2009/2010 pH1N1 pandemic in Montreal. The model accounted for heterogeneity in contact between

people in four different age groups. The effect of the summer school closure was also investigated. Daily humidity measures were allowed to affect the transmission of the virus. It was found that changing contacts and incorporating environmental humidity allowed for the two incidence waves to be recreated. We also estimated the level of disease underreporting for the four different age groups and between the first and second waves.